

AD-A010 144

THE EFFECTS OF USING UNPHASED SUBARRAY SUMS IN LASA BEAMS
ON THE DETECTION PERFORMANCE OF THE ARRAY

E. F. Chiburis, et al

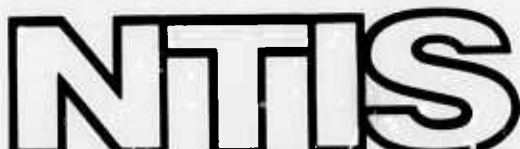
Teledyne Geotech

Prepared for:

Defense Advanced Research Projects Agency
Air Force Technical Applications Center

25 November 1974

DISTRIBUTED BY:



National Technical Information Service
U. S. DEPARTMENT OF COMMERCE

070	Edith Jenkins	<input checked="" type="checkbox"/>
071	Beth Jenkins	<input type="checkbox"/>
CERTIFICATION		
BY.....		
DISTRIBUTION/AVAILABILITY CODES		
Dist.	AVAIL. 01/01 SPECIAL	
		

Disclaimer: Neither the Defense Advanced Research Projects Agency nor the Air Force Technical Applications Center will be responsible for information contained herein which has been supplied by other organizations or contractors, and this document is subject to later revision as may be necessary. The views and conclusions presented are those of the authors and should not be interpreted as necessarily representing the official policies, either expressed or implied, of the Defense Advanced Research Projects Agency, the Air Force Technical Applications Center, or the US Government.

110)

Unclassified

SECURITY CLASSIFICATION OF THIS PAGE (When Data Entered)

REPORT DOCUMENTATION PAGE		READ INSTRUCTIONS BEFORE COMPLETING FORM
1 REPORT NUMBER SDAC-TR-74-14	2 GOVT ACCESSION NO.	3 RECIPIENT'S CATALOG NUMBER AD-A010 144
4 TITLE (and Subtitle) THE EFFECTS OF USING UNPHASED SUBARRAY SUMS IN LASA BEAMS ON THE DETECTION PERFORMANCE OF THE ARRAY		5 TYPE OF REPORT & PERIOD COVERED Technical
7 AUTHOR(s) Chiburis, E. F.; Ahner, R. O; Chang, A. C.		6 PERFORMING ORG. REPORT NUMBER F08606-74-C-0006
9 PERFORMING ORGANIZATION NAME AND ADDRESS Teledyne Geotech 314 Montgomery Street Alexandria, Virginia 22314		10 PROGRAM ELEMENT PROJECT TASK AREA & WORK UNIT NUMBERS
11 CONTROLLING OFFICE NAME AND ADDRESS Defense Advanced Research Projects Agency Nuclear Monitoring Research Office 1400 Wilson Blvd., Arlington, Virginia 22209		12 REPORT DATE 25 November 1974
14 MONITORING AGENCY NAME & ADDRESS (If different from Controlling Office) VELA Seismological Center 312 Montgomery Street Alexandria, Virginia 22314		13 NUMBER OF PAGES 50
16 DISTRIBUTION STATEMENT (of this Report) APPROVED FOR PUBLIC RELEASE; DISTRIBUTION UNLIMITED.		15 SECURITY CLASS. (of this report) Unclassified
		15a DECLASSIFICATION DOWNGRADING SCHEDULE
17 DISTRIBUTION STATEMENT (of the abstract entered in Block 20, If different from Report)		D D C DRAFTING MAY 28 1975 RELEASER D
18 SUPPLEMENTARY NOTES Reproduced by NATIONAL TECHNICAL INFORMATION SERVICE U.S. Department of Commerce Springfield VA 22151		
19 KEY WORDS (Continue on reverse side if necessary and identify by block number) LASA Seismic Detection Array Evaluation Beamforming		
20 ABSTRACT (Continue on reverse side if necessary and identify by block number) From mid-January 1974 through March, two sets of LASA A-D ring beams were formed in parallel by the on-line LASA Detection Processor (DP at SDAC). One set contained 299 LASA array beams using phased subarray sums; the other contained array beams to the same 299 regions using unphased subarray sums. In six experiments we used seismograms recorded by the inner 1, 4, 7, 10, 13 and all 16 sensors per subarray to form the unphased sums for the LASA beams. Each of the LASA beams so constituted was compared to the LASA beam containing		

Unclassified

SECURITY CLASSIFICATION OF THIS PAGE(When Data Entered)

phased sums of 16 traces per subarray. The objective of these experiments was to determine the effect on array detection performance of using unphased sums.

A comparison of the signal-to-noise (S/N) ratios of the on-line detections from the parallel beam sets shows that the average S/N loss on the beams containing unphased subarray sum traces varies from 2.4 db for 16 channels to 5.6 db for one channel. This suggests a change in threshold varying between 0.1 and 0.3 magnitude units; and the relative numbers of events detected by the phased and unphased subarray beams support this interpretation. This is, however, an average over the teleseismic distance range; the loss is greater for close-in distances than for large distances and is partly due to higher noise levels because of the smaller number of sensors in the smaller subarray. Separation and discussion of these two effects as a function of frequency leads to the conclusion that 10 sensors per subarray strikes a satisfactory balance between high-frequency signal loss and reduction of the detection threshold. There is, however, no sharp change at any particular number of elements, and other choices are possible.

ii

Unclassified

SECURITY CLASSIFICATION OF THIS PAGE(When Data Entered)

THE EFFECTS OF USING UNPHASED SUBARRAY SUMS
IN LASA BEAMS ON THE DETECTION PERFORMANCE OF THE ARRAY

SEISMIC DATA ANALYSIS CENTER REPORT NO.: SDAC-TR-74-14

AFTAC Project No.: VELA VT/4709

Project Title: Seismic Data Analysis Center

ARPA Order No.: 1620

ARPA Program Code No.: 3F10

Name of Contractor: TELEDYNE GEOTECH

Contract No.: F08606-74-C-0006

Date of Contract: 01 July 1974

Amount of Contract: \$2,237,956

Contract Expiration Date: 30 June 1975

Project Manager: Royal A. Hartenberger
(703) 836-3882

P. O. Box 334, Alexandria, Virginia 22314

APPROVED FOR PUBLIC RELEASE; DISTRIBUTION UNLIMITED.

iii

D D C
REFINED
MAY 28 1975
REGULATED
D

ABSTRACT

From mid-January 1974 through March, two sets of LASA A-D ring beams were formed in parallel by the on-line LASA Detection Processor (DP at SDAC). One set contained 299 LASA array beams using phased subarray sums; the other contained array beams to the same 299 regions using unphased subarray sums. In six experiments we used seismograms recorded by the inner 1, 4, 7, 10, 13, and all 16 sensors per subarray to form the unphased sums for the LASA beams. Each of the LASA beams so constituted was compared to the LASA beam containing phased sums of 16 traces per subarray. The objective of these experiments was to determine the effect on array detection performance of using unphased sums.

A comparison of the signal-to-noise (S/N) ratios of the on-line detections from the parallel beam sets shows that the average S/N loss on the beams containing unphased subarray sum traces varies from 2.4 db for 16 channels to 5.6 db for one channel. This suggests a change in threshold varying between 0.1 and 0.3 magnitude units; and the relative numbers of events detected by the phased and unphased subarray beams support this interpretation. This is, however, an average over the teleseismic distance range; the loss is greater for close-in distances than for large distances and is partly due to higher noise levels because of the smaller number of sensors in the smaller subarray. Separation and discussion of these two effects as a function of frequency leads to the conclusion that 10 sensors per subarray strikes a satisfactory balance between high-frequency signal loss and reduction of the detection threshold. There is, however, no sharp change at any particular number of elements, and other choices are possible.

TABLE OF CONTENTS

	Page
ABSTRACT	
INTRODUCTION	1
THRESHOLD CHANGES	5
THEORETICAL SUBARRAY SIGNAL RESPONSE	8
EXPERIMENTAL RESULTS AS A FUNCTION OF WAVELENGTH, PERIOD AND VELOCITY	9
SUMMARY AND RECOMMENDATIONS	13
REFERENCES	14
APPENDIX	

LIST OF TABLES

Table No.	Title	Page
I	Subarray sensor configurations and duration of on-line experiments	15
II	Summary of phased versus unphased subarray sum experiments	16
III	Comparison of theoretical and observed signal and noise loss at $\lambda = 15.5$ km.	17

LIST OF FIGURES

Figure No.	Title	Page
1	Array response for infinite velocity beam for the 4-inner elements of LASA subarray A0.	18
2	Array response for infinite velocity beam for all 16 elements of LASA subarray A0.	19
3	Theoretical array response for infinite velocity beam of the inner 4-16 elements of LASA subarray A0 averaged over azimuth. The mean and standard deviation are indicated. Also shown by dashed lines is the mean db difference in response between a 15.5 km/sec beam directed at the event azimuth and an infinite velocity beam.	20
4	Theoretical phase response for 4-16 sensors of the A0 subarray as a function of wavelength and azimuth of approach.	21
5	Array response for infinite velocity beams for the inner 4-16 elements of LASA subarray A0 averaged over azimuth as a function of normalized wavelength, λ/D .	22
6	Theoretical signal loss for unphased sums as a function of number of sensors per subarray for several periods and for $\Delta = 30^\circ$.	23
7	Theoretical signal loss for unphased sums as a function of number of sensors per subarray for several periods and for $\Delta = 60^\circ$.	24
8	Theoretical signal loss for unphased sums as a function of number of sensors per subarray for several periods and for $\Delta = 90^\circ$.	25
9	Signal-to-noise ratio loss in db as a function of apparent signal wavelength for experiment 1. The solid line is the (constant) array response of a single element shifted down until it passes through the median db point in the wavelength interval 12-18 km. The dashed line shows the response relative to a 15.5 km/sec beam directed at a 1 Hz signal.	26

LIST OF FIGURES (Continued)

Figure No.	Title	Page
10	Signal-to-noise ratio loss in db as a function of apparent signal wavelength for experiment 2. The solid line is the array response of the inner 4 elements shifted down until it passes through the median db point in the wavelength interval 12-18 km. The dashed line shows the response relative to a 15.5 km/sec beam directed at a 1 Hz signal.	27
11	Signal-to-noise ratio loss in db as a function of apparent signal wavelength for experiment 3. The solid line is the array response of the inner 7 elements shifted down until it passes through the median db point in the wavelength interval 12-18 km. The dashed line shows the response relative to a 15.5 km/sec beam directed at a 1 Hz signal.	28
12	Signal-to-noise ratio loss in db as a function of apparent signal wavelength for experiment 4. The solid line is the array response of the inner 10 elements shifted down until it passes through the median db point in the wavelength interval 12-18 km. The dashed line shows the response relative to a 15.5 km/sec beam directed at a 1 Hz signal.	29
13	Signal-to-noise ratio loss in db as a function of apparent signal wavelength for experiment 5. The solid line is the array response for the inner 13 elements shifted down until it passes through the median db point in the wavelength interval 12-18 km. The dashed line shows the response relative to a 15.5 km/sec beam directed at a 1 Hz signal.	30
14	Signal-to-noise ratio loss in db as a function of apparent signal wavelength for experiment 6. The solid line is the array response of the inner 16 elements shifted down until it passes through the median db point in the wavelength 12-18 km. The dashed line shows the response relative to a 15.5 km/sec beam directed at a 1 Hz signal.	31
15	Signal-to-noise loss in db as a function of signal period for 9 distance intervals for experiment 4; 10 sensors per subarray. Line has been transformed from dashed line in Figure 12 by assuming loss at period T is equal to loss at $\lambda = vT$ where v is the wave velocity appropriate to the distance.	32

LIST OF FIGURES (Continued)

Figure No.	Title	Page
16	Signal-to-noise loss in db as a function of signal period for 9 distance intervals for experiment 6; 16 sensors per subarray. The dashed line has been transformed from the dashed line in Figure 14 by assuming loss at period T is equal to loss at $\lambda = vT$ where v is the wave velocity appropriate to the distance.	33
17	Plots of the signal-to-noise ratio losses for LASA beams containing unphased subarray sums as compared to those made up of phased subarray sums for each event versus epicentral distance for each experiment. Both regression lines and transformed dashed lines from Figures 9-14 with $f = 1.0$ have been drawn through the data. Transformation effected by assuming loss at distance Δ is equal to loss at $\lambda = vT$, $T = 1.0$, v as appropriate according to distance.	34
18	Signal-to-noise ratio loss for $\Delta = 30^\circ$ as a function of number of sensors per subarray for several frequencies. Taken from transformations of the dashed lines in Figures 9-14.	35
19	Signal-to-noise ratio loss for $\Delta = 60^\circ$ as a function of number of sensors per subarray for several frequencies. Taken from transformations of the dashed lines in Figures 9-14.	36
20	Signal-to-noise ratio loss for $\Delta = 90^\circ$ as a function of number of sensors per subarray for several frequencies. Taken from transformations of the dashed lines in Figures 9-14.	37

INTRODUCTION

The objective of this study is to determine the effects of using unphased subarray sums on the detection and discrimination performance of the Large Aperture Seismic Array (LASA) in Montana and to make preliminary recommendations of the number of sensors to use to form the unphased sums.

It is anticipated that the 50 kilobit line capability from Montana to the SDAC will be reduced to a 4.8 kilobit line in the near future. To conform to this reduced transmission rate, the data output from LASA can be decreased by transmitting unphased subarray sums from Montana from each of the thirteen remaining subarrays instead of transmitting the individual outputs from the 208 sensors still in operation.

As programmed for this experiment, the detection process in Partition I serves as a base of comparison for the unphased sums (calculated in Partition II). In Partition I we form five 16-sensor subarray phased sums equi-spaced in azimuth at a velocity of 15.5 km/sec (0.0645 sec/km) for each of the thirteen subarrays. The subarray beams are combined into the full array beamset LBS 140 which selects from each subarray the beam which is closest in velocity space to the beaming point of the full array beam. The 299 beaming points in the full array beam are hexagonally packed in inverse velocity space with a spacing of 0.001316 sec/km out to a radius of 0.132 sec/km or 7.6 km/sec.

These beams are then examined by a detection process described by Chang (1974). For ease of reference, we shall briefly review the process.

The subarray beams in this experiment have been filtered 0.8-2.5 Hz instead of 0.9-1.4 Hz as was previously implemented in the SDAC system. Because of the broader pass-band, pulse-like signal wave-forms are not so extended in time after passing through the filter.

This fact suggests that changes in other detection parameters might be desirable. Such changes were made and are discussed below. The first step in detection is to accumulate a short-term average (STA) of the noise by averaging over 1.8 seconds of the rectified beam of interest. Successive

overlapping STA values are computed every 0.6 seconds. From these STA's a long-term average is computed every third step, or once in 1.8 seconds, by exponentially weighting the previous LTA value and adding the current STA value. The detection algorithm tests if the STA/LTA ratio is greater than a S/N acceptance threshold (10 db in these experiments) each time an STA is computed.

There are two parts to the detection algorithm for LASA. The first part is the signal to noise ratio (S/N) threshold test which determines the size and duration of the signal. When the ratio of the STA/LTA exceeds the fixed threshold value of 10 db for the duration of Q out of Q' (2/2 in the experiment; changed from 3/3 as previously implemented) consecutive tests, the signal arrival is declared "on" on that beam. After the beam is turned on, the end of the signal arrival is declared when the S/N ratio of the beam becomes lower than the turn-off threshold of 7 db. The LTA computation is stopped when the beam is "on". Note, however, that the LTA may be contaminated by the signal because if the LTA is being updated at the first successful threshold test (one chance in three), then the STA being added to the LTA will contain some signal. (While this should not affect detection thresholds since weak events cannot significantly affect the LTA, it will lower the reported S/N values for large events one-third of the time.)

The second part of the detection algorithm is the spatial consistency test. This determines the consistency of the seismic signal in both azimuth and velocity by seeking the maximum STA beam and checking if the previous maximum was found within the distance of ΔU beams ($\Delta U = 2$ beams) from the current maximum beam. When this condition is satisfied for P (P = 3 in this experiment; changed from 4 as previously implemented) consecutive times, the signal arrival is declared on the beam with the highest STA value during these P consecutive tests. If that beam is "on" by virtue of having passed the threshold test then both parts of the detection algorithm have been passed and a detection is declared.

To carry out our experiments, this detection system was placed in Partition I of the SDAC system. In Partition II we placed an identical system

except that only one beam, an infinite velocity beam, was formed at the subarray level; and a variable number of sensors were summed into the subarray beam depending on the experiment under consideration as illustrated in Table I.

The complete printed Detection Processor (DP) outputs are available for both partitions; and we have compared the number of events which crossed the 12 db threshold and were confirmed by the analysts in the two partitions. As it happened there was never a case of a detection above 12 db in Partition II and not in Partition I which was accepted as an event by the analysts. Thus we have tabulated the percentage of analyst-accepted Partition I events above 12 db which were also detected in Partition II above 12 db. We have also tabulated the difference in (S/N) for all accepted events with (S/N) greater than 10 db in Partition II. This is as low as it is possible to tabulate because lower db values are not printed out.

No comparison was made of the false alarm rate between the two partitions; however, there is every reason to expect that they would be identical. By reference to Blandford and Clark (1971) the intersensor noise correlation inside a subarray is very low in the 0.8-2.0 Hz pass-band for both infinite velocity and 12 km/sec beams. The noise correlation between subarrays is generally regarded as zero, and in general one does find \sqrt{N} noise reduction by beamforming subarrays, Hartenberger and van Nostrand (1970). Thus, no matter what the subarray beam, and no matter how many sensors in the subarray, one expects the noise processes to be identical among partitions and among experiments except for the mean-square level. The mean-square level will, however, not affect the false alarm rate since the threshold is a relative one; comparing a short-term average of the noise to a long-term average. Examination of a day's DP output: February 20, 1974 showed no difference between partitions in the number of threshold crossings flagged by the event processor as sidelobe detections or as later phase arrivals. In any event, such an increase would result in no increased load on the analysts.

It would have been possible to run each experiment on the same data by use of the off-line DP system. If this had been done, a more controlled

comparator would have been possible between experiments. Unfortunately the off-line DP runs at one-half real time; and the 360/40B required for the off-line runs is available only 6 hours per day on the average. Thus to run the same number of experiments would have required eight times as long; or 2-3 years instead of 3-4 months, see Table I. Off-line DP tests also encounter severe tape reading problems, Chiburis et al. (1974).

The required results could also have been obtained at very low computation cost simply by beamforming a few large events for each distance interval and region of interest. Experience has shown that the standard deviation of signal-to-noise improvement estimates obtained by this method is very low; and that only a few events are needed to define the mean. (In contrast, of course, a very large number of events are required to accurately determine a threshold by the technique of plotting probability of detection or number of detections versus magnitude.)

However, it is desired to test the actual system in operation so that any unsuspected effects of the complicated detection algorithms just discussed would be revealed.

THEORETICAL CHANGES

In Table II we see some of the principal results of experiments 1-6. We see in Table I that the subarrays were filled from the center out as the number of the experiment increased. It would seem that these are the subarray designs of interest since in this way the signal loss on unphased sums due to signal misalignment, and the costs of cable and instrument maintenance increase monotonically. Also, as we shall see, the most closely spaced sensors contribute in all subarray designs to reduction of noise. (It is of interest in this regard that the original array design of the Geneva experts called for an array of 3 km diameter because zero-delay analog summation of the individual sensors was envisaged as the processing scheme of choice.)

In each of the experiments the average distance to the events lay between 63°-70° with a mean of 67°; and the average waveform period in each experiment was 0.9 seconds. To the extent that the stability of these statistics indicates that the sample populations range of 113-379 events can be taken as a satisfactory sample of the population of interest, we may obtain a crude estimate of the threshold change from the percent detection in the second partition.

It is generally assumed that the probability of detection is a function of the signal-to-noise ratio, that is to say a function of the difference in the logarithm of the signal and noise. Blandford and Wirth (1973) have shown that this function may be approximated for automatic detectors by a step from 0 to 1.0 probability at specified (S/N). Then, for any particular array, the probability of detection is equal to the probability of attaining a (S/N) value greater than a particular threshold value. For a fixed LASA magnitude at a fixed distance, the magnitude is proportional to the log amplitude. Since the mean noise amplitudes have been found by many workers to be distributed log-normally, the probability of detection of a fixed m_b is given by

$$p(m_b - \mu) = p((m_b - \mu)/2\sigma) = \phi((m_b - \mu)/2\sigma)$$

where $\mu = B(\Delta) + \log a + \log r$ combines the logarithm of the (S/N) threshold value r ; the logarithm of a , the median noise level; and $B(\Delta)$ the distance

amplitude factor for P waves; σ is the standard deviation of the log noise and ϕ is the cumulative normal distribution function. If we neglect the variation of log amplitude with distance for fixed m_b for the events in the LASA detection list we may use the above formula for all events.

Then if the number of events with magnitude m_b is given by

$$n = C 10^{-bm_b}$$

then the total number of detected events is

$$N = C \int_{-\infty}^{\infty} p(m_b - \mu) 10^{-bm_b} dm_b$$

and a transformation of the variable of integration $\eta = m_b - \mu$ shows that:

$$\frac{N(\mu_1)}{N(\mu_2)} = 10^{-b(\mu_1 - \mu_2)}.$$

Thus if we know b , then from the change in percent events detected in Partition II compared to those in Partition I, we can determine the change in the "effective" threshold.

From Figure 8 in Chang (1974), the cumulative recurrence curve for 1500 LASA EP amplitudes we obtain $b = 1.06$; from Dean (1971) we obtain $b = 0.9$ from a recurrence curve of 500 LASA m_b values. Let us choose $b = 1.0$. By application of the above analysis, we arrive at column d in Table II.

To determine the (S/N) loss in each experiment we averaged the difference in log (S/N) in each partition for all events detected in Partition II above 10 db. These results are also given in Table II and we see that they are in good agreement with the results obtained from the relative number of events detected. It must be remembered however that this is a crude comparison as we have included in each average low frequency events from 90° and high frequency events from 20° whose losses, as we shall see, are greatly different. Also, in subsequent sections, we shall uncover substantial biases in the data. Finally we are comparing the infinite velocity beams to a LASA beam set which has, as of this writing, been substantially

improved by the addition of an infinite velocity subarray beam, together with a redistribution of the outer 5 subarray beams to better cover short wavelengths. Thus the losses in Table II are less than would be observed in a comparison with this improved beam set.

Much of the change in threshold is, of course, due to the changes in noise reduction as the number of elements in each subarray changes. To evaluate the effects of signal loss as a function of frequency on discrimination using, e.g., cepstral analysis or spectral ratios (0.4-0.8 Hz/1.4-1.8 Hz), it is necessary to allow for this noise loss reduction. In the following section we shall discuss the signal loss as a function of frequency from a theoretical point of view; and show that, when combined with the expected noise reduction, and with allowance made for effects of bias, the predicted S/N loss is in agreement with the results given in Table II, and with plots of the data presented in other ways. Thus we will be able to give theoretical estimates of signal and noise loss which are compatible with the data and which enable us to make estimates of the potential losses in detection and discrimination which will result from the formation of unphased sums for subarray beams.

THEORETICAL SUBARRAY SIGNAL RESPONSE

In Figures 1 and 2 we see that the array response out to $K_x = K_y = 0.143$ (7.0 km wavelength, $1/K = \lambda = v/f$) of the A0-16 and 4 element subarrays. We see that the response is almost perfectly circular, a fact which is emphasized by Figure 3 which shows the mean and standard deviation of the array responses for 4, 7, 10, 13 and 16 elements averaged over azimuth. Formulas for the array response are given in the Appendix. Also in Figure 3 the dashed lines give the loss at 1 Hz relative to a 15.5 km/sec beam directed to the proper azimuth.

In Figure 4 we see the phase response for the unphased sums (infinite velocity subarray beam) for each experiment as a function of signal wavelength and azimuth of approach. Only angles from 0-60° are plotted since the response should be periodic because of the hexagonal symmetry of all the subarray designs.

As a sidelight it is of interest that all the amplitudes responses are similar if normalized by the maximum intersensor spacing. This result is shown in Figure 5.

Figures 6, 7 and 8 give the mean signal loss of the unphased sums as a function of array size and period for the event distances 30°, 60°, and 90° respectively. We see that for the periods plotted the signal distortion would not be great in the AI at a distance of 90°, but that a distance of 30°, any subarray larger than 4 elements would strongly distort the spectrum and raise the threshold of any discriminant requiring high-frequency information, e.g. a cepstral depth estimate, by 0.2-0.3 more magnitude units.

EXPERIMENTAL RESULTS AS A FUNCTION OF WAVELENGTH, PERIOD AND VELOCITY

Figures 9 through 14 give the signal to noise loss as a function of wavelength for experiments 1-6 respectively. The wavelength was calculated by the formula $\lambda = v/f = vT$ where v is determined by standard tables from the distance to the event, and where T is the reported period for the event. Superimposed on these figures is the theoretical mean array response from Figure 3, displaced downwards so that it passes through the median point in the interval 12-18 km. This wavelength interval was chosen because the Partition I subarray beams were set at a velocity of 15.5 km/sec ($\lambda = 15.5$ km at 1.0 Hz), and thus the loss of the unphased sums at this velocity should be the true loss relative to a perfectly formed subarray beam. This will be in error by less than 1 db because of the slight average error in azimuth for the closest subarray beam. (This median loss is tabulated in column 4 of Table III.) The vertical shift of the solid curves in Figures 9-14 then represents the estimated relative noise reduction for this array, and the curves then gives the S/N loss (instead of the signal loss) expected at all wavelengths relative to a perfectly formed beam.

Before a comparison can be made between theory and observations, however, allowance must be made for the fact that the subarray beams in Partition I are not perfectly in phase for very low and very high velocity events. We have, therefore, shown a second line in Figures 9-14 which corrects for the db difference of the loss due to the unphased sums (infinite velocity beam) and that of the 15.5 km/sec beam. This difference curve is tangent to the unphased sum (infinite velocity) loss curve at 15.5 km/sec since the 15.5 km/sec beam has zero loss there, and the difference at other wavelengths is also equal to the difference in Figure 3.

We see that for 10-16 elements per subarray (Experiments 4-6, Figures 12-14) the differential response line falls below the data points for $7 \leq \lambda \leq 10$. This is as would be expected due to the substantial loss in S/N for low-wavelength events on infinite velocity beams which results in their not being detected at all in Partition II, and therefore results in their not being plotted at all on the Figures. Thus we see that the data as presented have

a substantial bias at low wavelengths, and simple extrapolation or interpretations could lead to substantial errors in judgment.

For 4-7 sensors per subarray (Experiments 2, 3; Figures 10, 11) the differential response matches the data points satisfactorily; suggesting that the small differential loss of about 4 db leads to little bias.

This line of argument leads one to expect that the data points would cluster about the differential line for 1 sensor per subarray (Experiment 1, Figure 9) instead of falling below it as observed. The only explanation we can give for this behavior is that the reflection from the free surface arriving at the 500 foot deep seismometer is more out of phase with the direct arrival than it is at the 200 foot deep seismometers. The effect will be largest for the high frequency events at large incidence angles (low velocities); i.e., those from close in.

Figure 9 also offers an opportunity to evaluate the effects of signal contamination of the noise, the possibility of which is discussed in the INTRODUCTION. The effect should be greatest in experiment 1 where the difference in S/N ratio between partitions is also the greatest. On Figure 9 we have indicated that the median value of S/N loss for all events, for those for which the S/N in Partition I was less than 20 db, greater than 20 db, and greater than 32 db was 5.6, 5.2, 5.8 and 5.8 db respectively. Thus it would appear that with respect to the overall average, bias from noise contamination is ≤ 0.2 db, a negligible effect.

As we have seen, however, the bias due to non-detection at low wavelengths has a major effect in the data for 10, 13 and 16 elements per subarray, and this fact is reflected in Figures 15 and 16 for 10 and 16 elements per subarray respectively where as a result of the bias the full range of the variation of S/N loss with period cannot be seen. Still, it is clear in the case of 16 elements per subarray that for $10^\circ < \Delta < 50^\circ$ there is a substantial increase in signal loss with frequency, and that this increase is in substantial agreement with the losses predicted from transformations of the dashed line in Figure 14, when allowance is made for the effects of bias.

Similarly, in Figure 17 we see that regression lines are in good agreement with the theoretical lines from Figure 9-14 evaluated at 1.0 Hz except at short distances where the effects of bias become important.

Figures 18-20 for $\Delta = 30^\circ$, 60° , and 90° respectively give the expected S/N loss relative to a perfectly formed subarray beam for 0.5, 1.0, 2.0 Hz as a function of number of sensors per subarray. These Figures, derived from the solid lines in Figures 9-14 correspond to the signal loss Figures 6-8. An example of the use of these Figures would be to consider the use of a short-period discriminant at a distance of 60° . From Figure 8 we see that for a 10-element array a short period 0.6 second spectral amplitude would have to be corrected upward by 4 db before computation of a spectral ratio; while by reference to Figure 20 we see that the threshold magnitude for application of the discriminant would have to be increased by about 7.5 db or .37 magnitude units. It is worth noting that the S/N loss relative to the 16-element array for 0.5 Hz is certainly overestimated because the noise correlation is higher at 0.5 Hz than in the band 0.8-2.5 Hz, thus giving the larger subarrays less of an advantage over the small.

The losses derived from Figures 6-8 and 18-20 are the ones to consider for planning purposes, since the new subarray beamset in LBS 151 now implemented at SDAC has 6 subarray beams including one unphased sum (infinite velocity). The full teleseismic velocity space out to 7 km/sec is covered with a maximum loss of 3 db at 1 Hz.

In Table III we give a careful comparison of our observed results with theory. In column 3 we give the theoretical signal loss for $\lambda = 15.5$ from Figure 3. In column 4 we give the observed S/N loss for $\lambda = 15.5$ from the db value at $\lambda = 15.5$ of the lines in Figures 9-14. The difference in these two columns is the apparent noise loss in the frequency band 0.8-2.5 Hz and is given in column 5.

The theoretical noise loss in the band 0.8-2.0 Hz may be found by the techniques discussed by Blandford and Clark (1971). Briefly, they used the observed correlation as a function of distance to compute δ , the average inter-sensor noise correlation for the array. Then the db noise reduction

is given by $10 \log_{10} (N/(1+[N-1]\rho))$. This technique applied to the subarray designs in this report gives the theoretical noise reduction in column 6. Since the noise spectrum at LASA is heavily dominated by low frequencies this result should be a good estimate of the noise reduction in the passband 0.8-2.5 Hz. Thus, subtracting column 6 from column 5 yields the theoretical minus apparent noise loss column 7. We see that the smaller the array the better it performs in comparison with theory; although the differences are only significant with respect to practice for the 1-sensor subarray.

Of the 3.9 db discrepancy for experiment 1 we can, as discussed above, explain only 0.2 db by appeal to (S/N) bias. Since the center element is buried 500 instead of 200 feet we may expect that its noise level is less than for the average other sensor. In fact, examination of Table 22 from Chiburis and Hartenberger (1966) shows that the average center sensor is quieter by 1.3 db than the average other sensor. This leaves 2.4 db to be accounted for. We feel that the probable explanation for the remaining discrepancy is that the travel-time residuals, computed either by examination of the single center-sensor trace or by cross correlation of the subarray beams (which are heavily dominated by the closely spaced sensors around the center element and which would be expected, no matter what the central concentration, to give an average residual close to the residual for the geometric center of the array) would be most representative of the array center sensors. The advantage would be expected to decrease as the size of the subarray increases; and this is, in fact, observed in Table III.

SUMMARY AND RECOMMENDATIONS

Figure 6-8, and 18-20 seem to be confirmed by comparison of their corollaries with observation. They may therefore be used to deduce the loss of signal, and signal-to-noise ratio as a function of frequency which would result from the formation of unphased sums in place of the present LASA beams which contains 6 subarray beams for each subarray.

It might be suggested that it would be desirable to lose less than $0.1 m_b$ unit detection threshold in the AI. Then by Figure 21 for $\Delta = 90^\circ$, $T = 1.0$ one would want to use 10 elements in each beam. The threshold for short-period spectral ratio ($T = 0.5$) discriminant would then be raised by about 0.2 magnitude units in the AI. At $\Delta = 60^\circ$ (Kamchatka, Novaya Zemlya, Tahiti) the corresponding numbers would be 0.15 and 0.4 magnitude units; while at 30° (Cuba, Guatemala, Bering Straits, Amchitka) we would have 0.2 and 0.5 magnitude units. These seem to be relatively reasonable results; there is no obvious break in any of the curves which would lead to an optimum via simple reasoning. Seven sensors per array also seems reasonable; but since it is easier to cut a sensor out of the beam than to add it, one might well be biased toward the higher number.

REFERENCES

- Blandford, R. R. and D. M. Clark, 1971. Seismic array design, Seismic Data Laboratory Report 267, Teledyne Geotech, Alexandria, Virginia.
AD 884 710
- Blandford, R. R. and M. H. Wirth, 1973. Automatic array and network detection in the presence of signal variability, Seismic Data Laboratory Report 308, Teledyne Geotech, Alexandria, Virginia. AD 768 927
- Chang, A. C., 1974. A comparison of the LASA-NORSAR short period arrays, Teledyne Geotech, SDAC Technical Report 74-5.
- Chiburis, E. F. and R. A. Hartenberger, 1966. Signal-to-noise ratio improvement by time-shifting and summing LASA seismograms, Seismic Data Laboratory Report 164, Teledyne Geotech, Alexandria, Virginia.
AD 800 370
- Chiburis, E. F., R. O. Ahner, A. C. Chang, and A. U. Kerr, 1974. The effects of reduced configurations at LASA on detection signal-to-noise ratios, SDAC Report TR-74-7, Teledyne Geotech, Alexandria, Virginia.
- Dean, W. C., R. O. Ahner, E. F. Chiburis, 1971. Seismic Array Analysis Center evaluation of the SAAC/LASA system, SAAC Report No. 1, Teledyne Geotech, Alexandria, Virginia.

TABLE I
Subarray Sensor Configurations and Duration of On-Line Experiments

<u>Experiment</u>	<u>Duration of Experiments (Year, month, day, GMT)</u>	<u>Approx. Days Duration</u>	<u>Subarray Sensors Configuration (Partition I)</u>	<u>Subarray Sensors Configuration (Partition II)</u>
1	740116/1343-740118/1644	11	16-phased sums 5 azimuths	1 - center sensor
2	740128/2010-740207/1605	10	16-phased sums 5 azimuths	4 - center and 3 inner sensor unphased sums
3	740207/1605-740215/1629	8	16-phased sums 5 azimuths	7 - center and 6 inner sensor unphased sums
4	740215/1629-740311/1919	24	16-phased sums 5 azimuths	10 - center and 9 inner sensor unphased sums
5	740311/1919-740321/1429	10	16-phased sums 5 azimuths	13 - center and 12 inner sensor unphased sums
6	740321/1429-740402/1357	12	16-phased sums 5 azimuths	16 - all sensors unphased sums

TABLE II
Summary of Phased versus Unphased Subarray Sum Experiments

<u>Experiment</u>	<u>Number of Sensors/Subarray</u>	<u>(a)</u>	<u>(b)</u>	<u>(c)</u>	<u>(d)</u>	<u>Average S/N Loss (db)</u>	<u>σ (dB)</u> <u>Single Observations</u>
1	1	148	67(45%)	12	6.9	5.6	1.7
2	4	175	112(64%)	13	3.8	3.9	1.4
3	7	113	84(74%)	10	2.6	3.3	1.2
4	10	379	263(69%)	33	3.3	2.7	1.3
5	13	135	106(79%)	10	2.0	2.4	1.5
6	16	238	117(74%)	19	2.6	2.4	1.5

- (a) No. of Events detected by the full LASA beams and with $S/N \geq 12$ db.
 - (b) No. of Events detected by LASA beams containing unphased subarray sums and with $S/N \geq 12$ db.
 - (c) No. of Events detected by LASA beams containing unphased subarray sums and with $S/N \geq$ between 10 and 12 db (included in S/N loss results).
 - (d) dB loss corresponding to $20 \times \Delta m_b$, where Δm_b is the log threshold loss calculated assuming $b = 1.0$.
- σ Standard deviation about the mean for S/N loss. To compute standard deviations of the mean of the S/N loss, divide σ by the square-root of number of events detected, (b) + (c).

TABLE III
Comparison of Theoretical and Observed Signal and Noise Loss at $\lambda = 15.5$ km

No. Sensors per Subarray	<u>Experiment</u>	Theoretical Signal Loss $\text{@ } \lambda = 15.5$	Observed S/N Loss @ $\lambda = 15.5$	Apparent Noise Loss		Theoretical Noise Loss 0.8-2.0 Relative to 16 Elements	Theoretical Apparent Noise Loss @ $\lambda = 15.5$
				(1)	(2)	(3)	(4)
1	1	.0	5.60	5.60	5.60	9.50	3.90*
4	2	0.60	4.20	4.20	3.60	4.75	1.15
7	3	1.00	3.50	3.50	2.50	3.00	.50
10	4	1.55	2.80	2.80	1.25	1.80	.55
13	5	2.00	2.40	2.40	0.40	.85	.45
16	6	2.50	2.35	2.35	-0.15	0.00	.15

* In Experiment (1) if we count 1.3 dB for the quiet center element at a depth of 500 feet, and 0.2 dB for (S/N) bias, the (theoretical-apparent) noise loss is reduced from 3.9 to 2.4 dB. Some of the remainder may be due to the fact that travel-time residuals are calibrated to the center element so that a beam of these elements will be better than a beam of other elements.

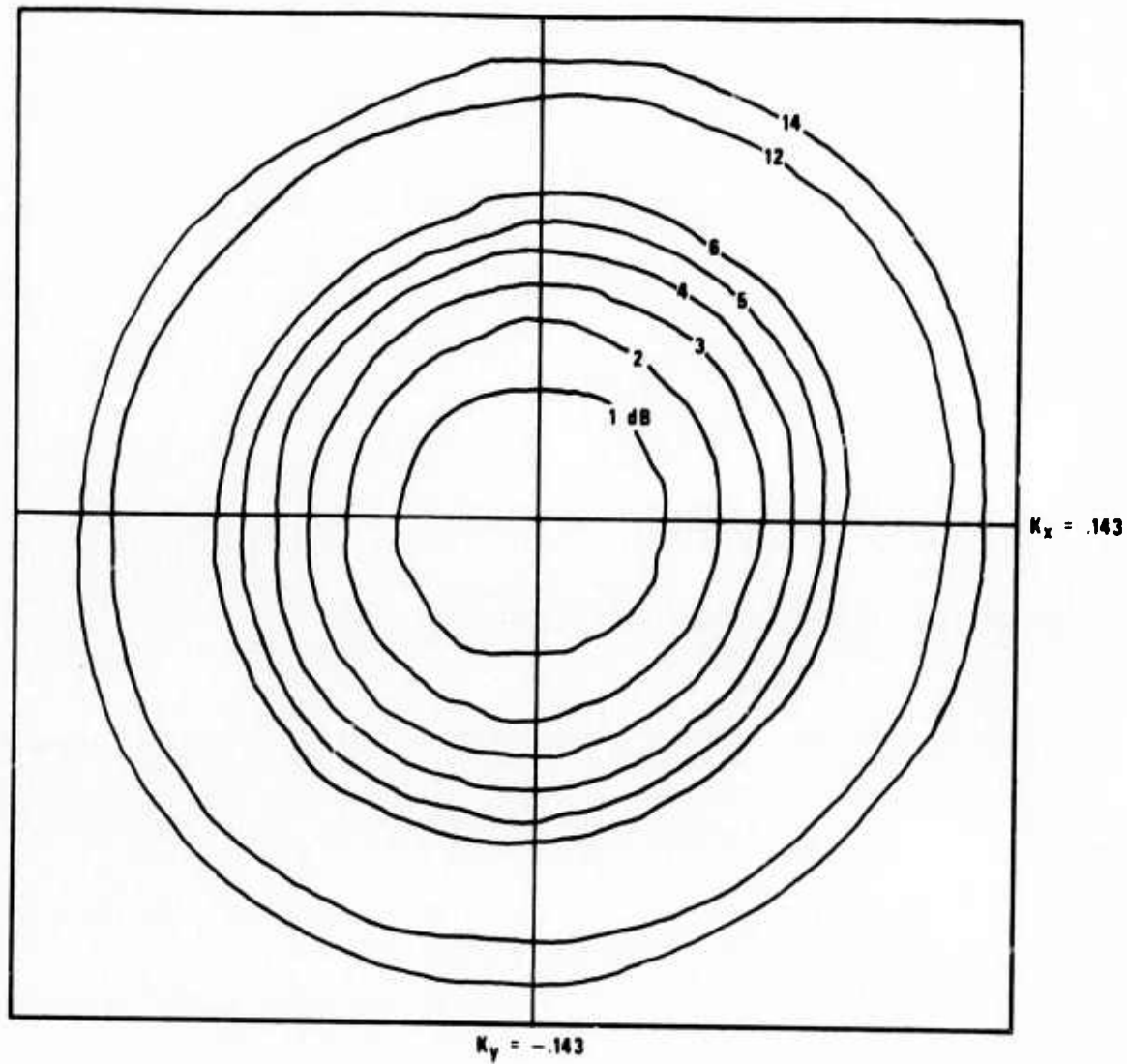


Figure 1. Array response for infinite velocity beam for the 4-inner elements of LASA subarray A0.

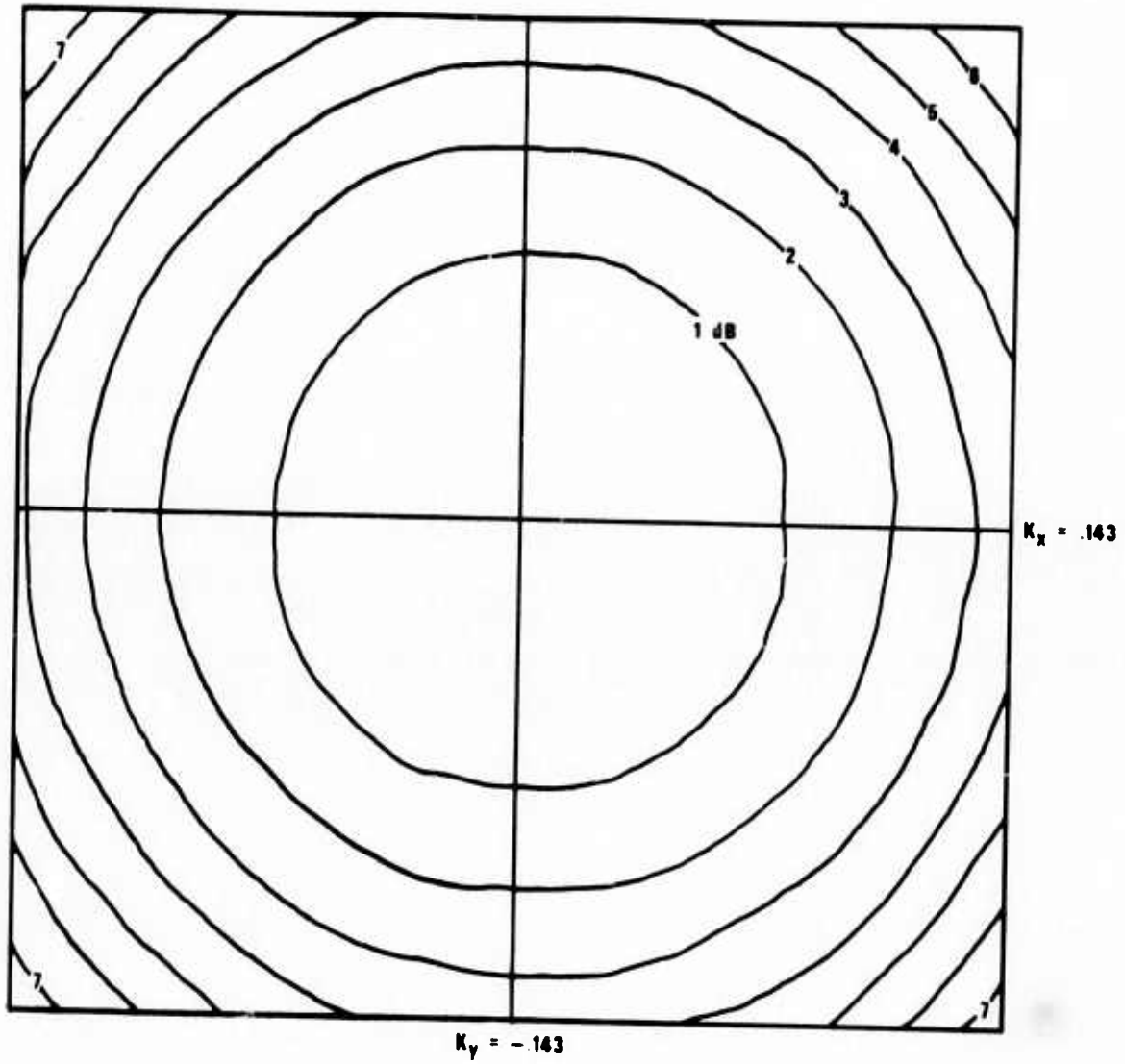


Figure 2. Array response for infinite velocity beam for all 16 elements of LASA subarray A0.

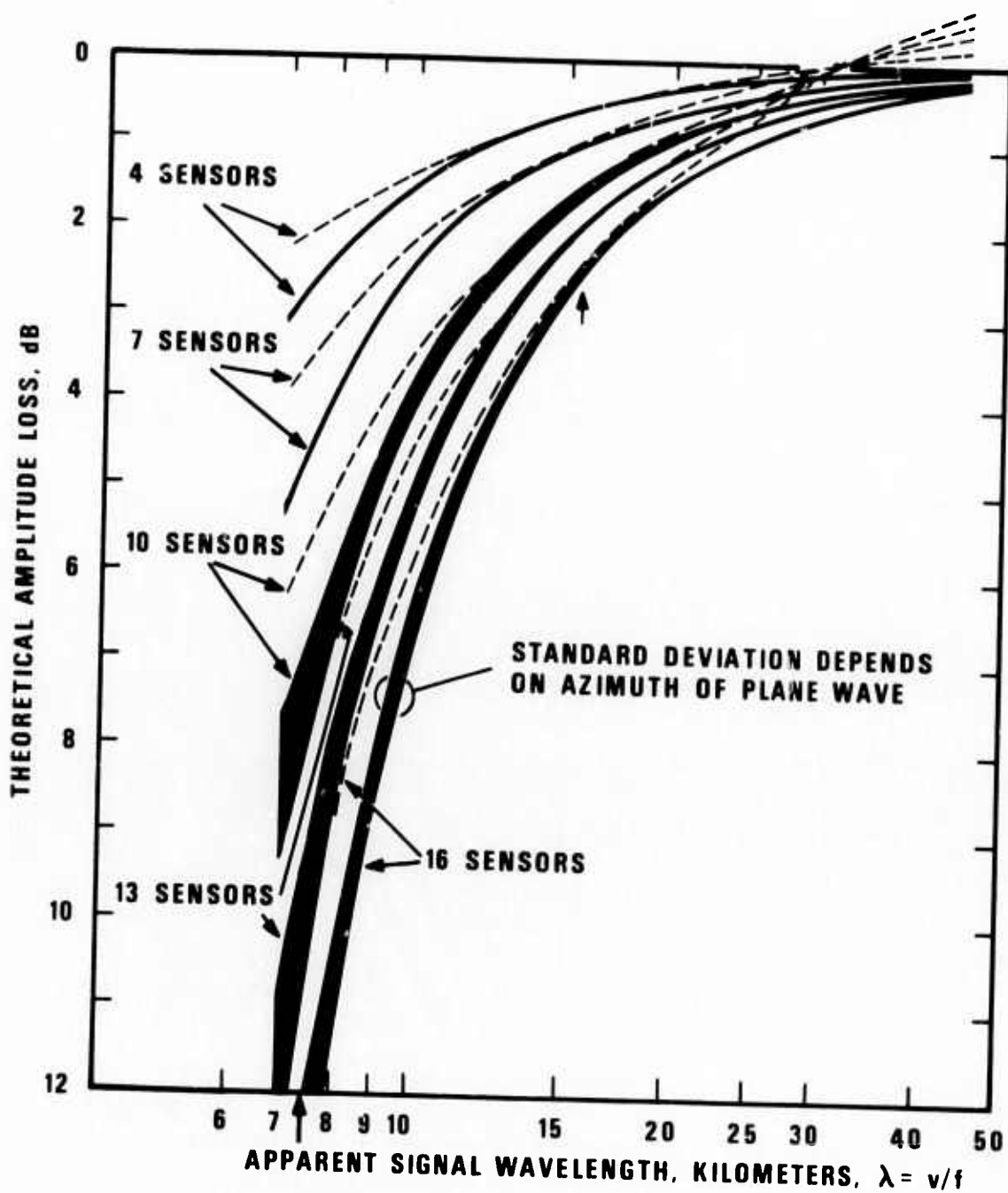


Figure 3. Theoretical array response for infinite velocity beam of the inner 4-16 elements of LASA subarray A0 averaged over azimuth. The mean and standard deviation are indicated. Also shown by dashed lines is the mean db difference in response between a 15.5 km/sec beam directed at the event azimuth and an infinite velocity beam.

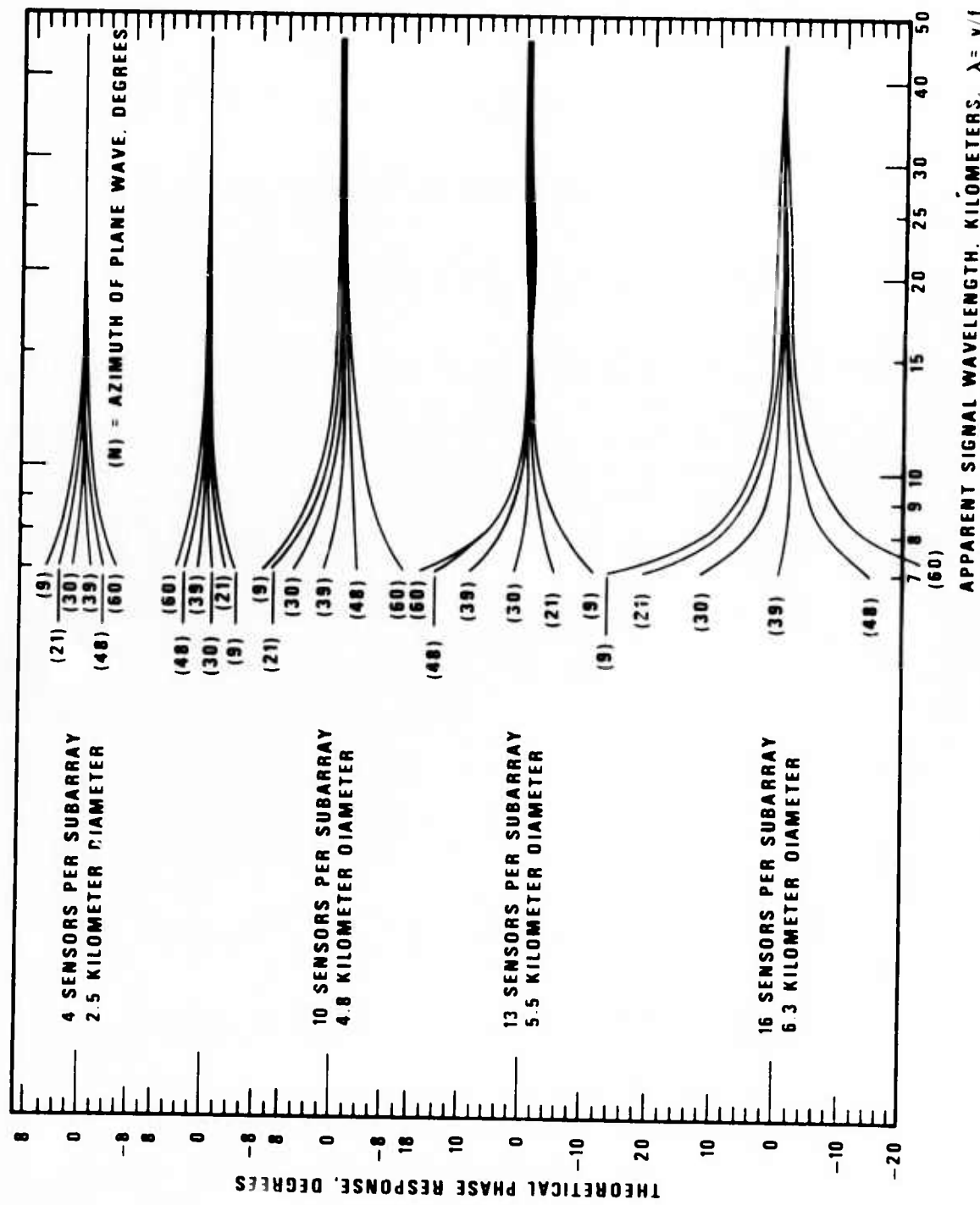


Figure 4. Theoretical phase response for 4-16 sensors of the A0 subarray as a function of wavelength and azimuth of approach.

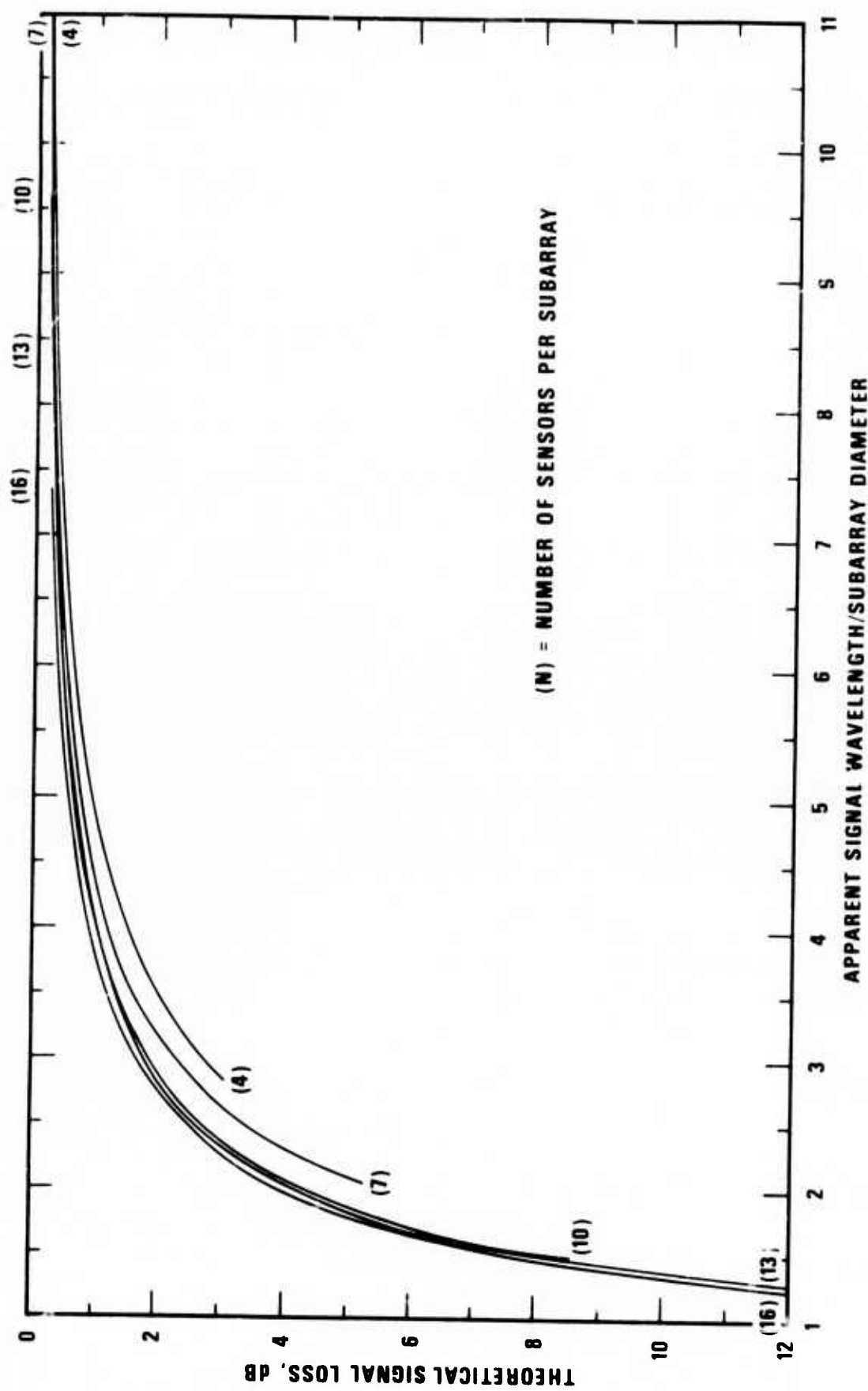


Figure 5. Array response for infinite velocity beams for the inner 4-16 elements of LASA subarray A0 averaged over azimuth as a function of normalized wavelength, λ/D .

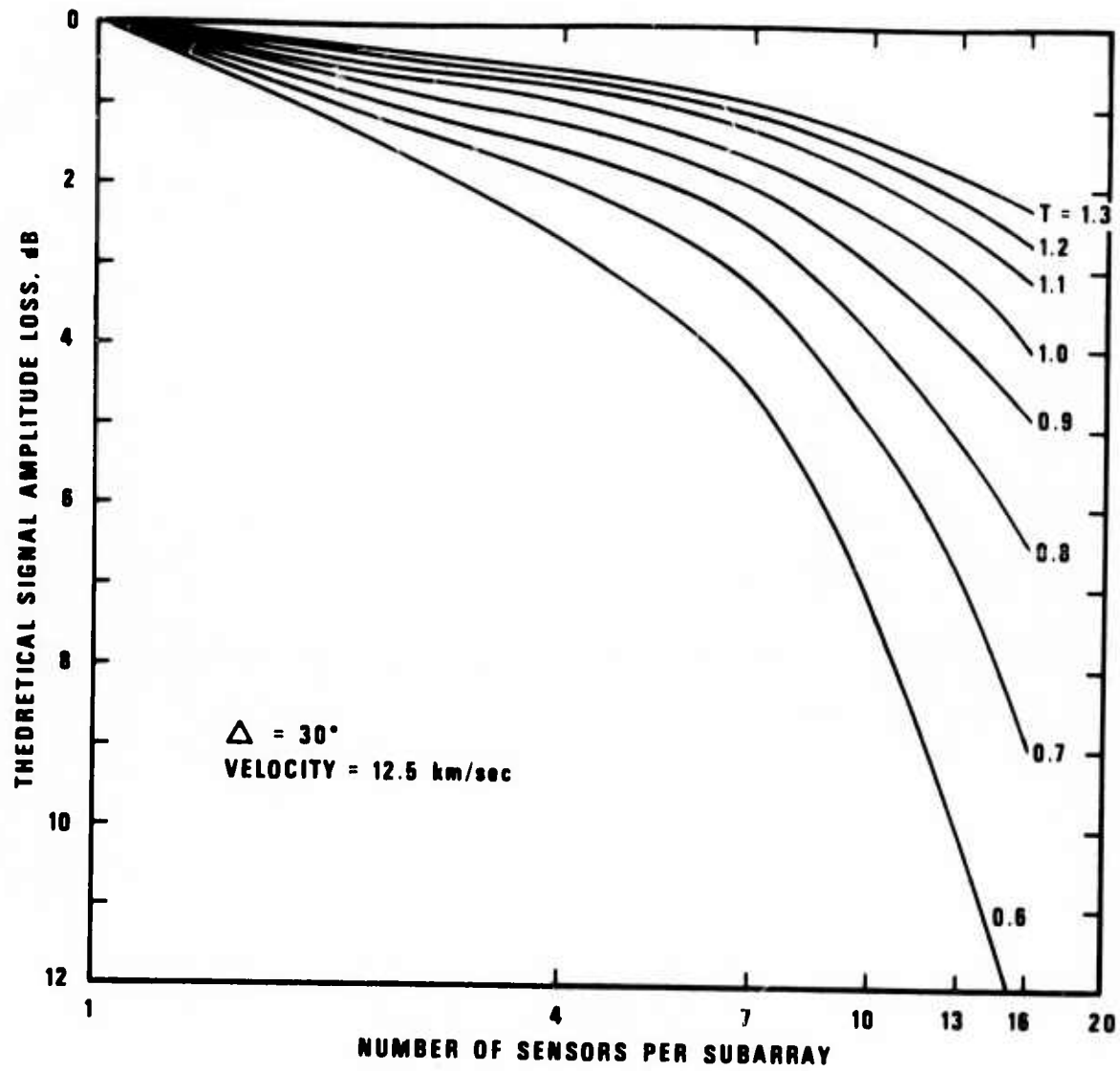


Figure 6. Theoretical signal loss for unphased sums as a function of number of sensors per subarray for several periods and for $\Delta = 30^\circ$.

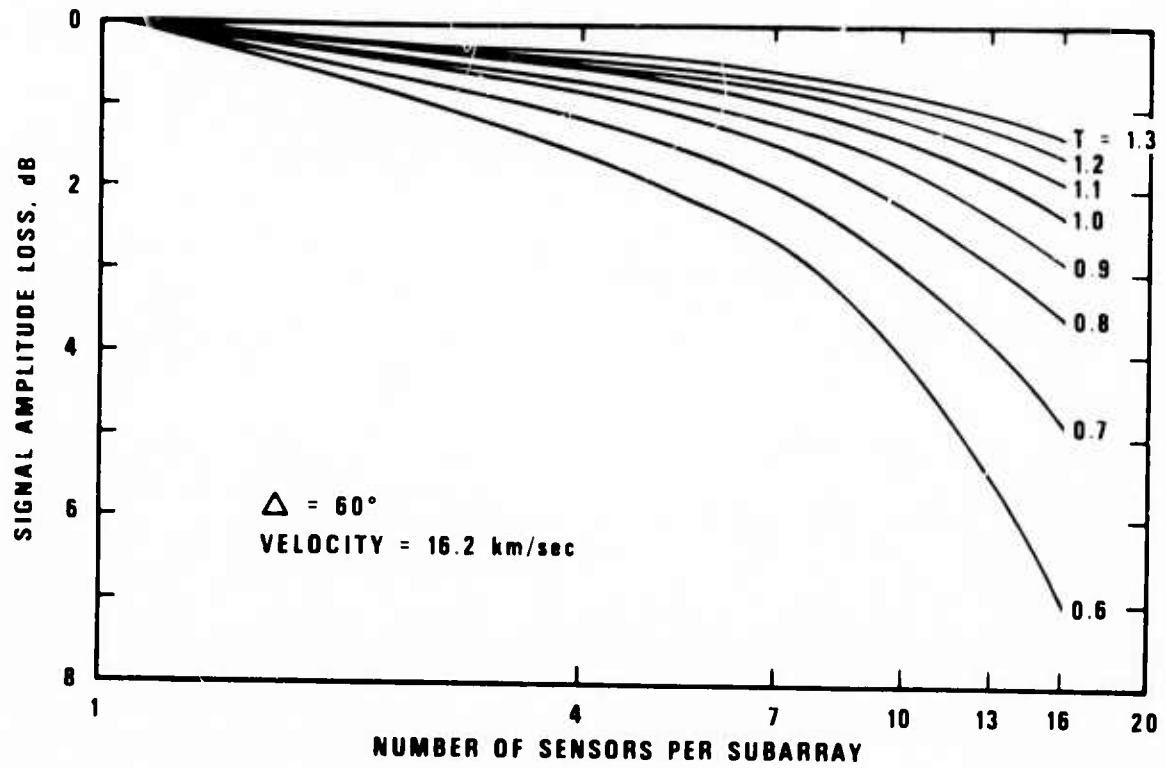


Figure 7. Theoretical signal loss for unphased sums as a function of number of sensors per subarray for several periods and for $\Delta = 60^\circ$.

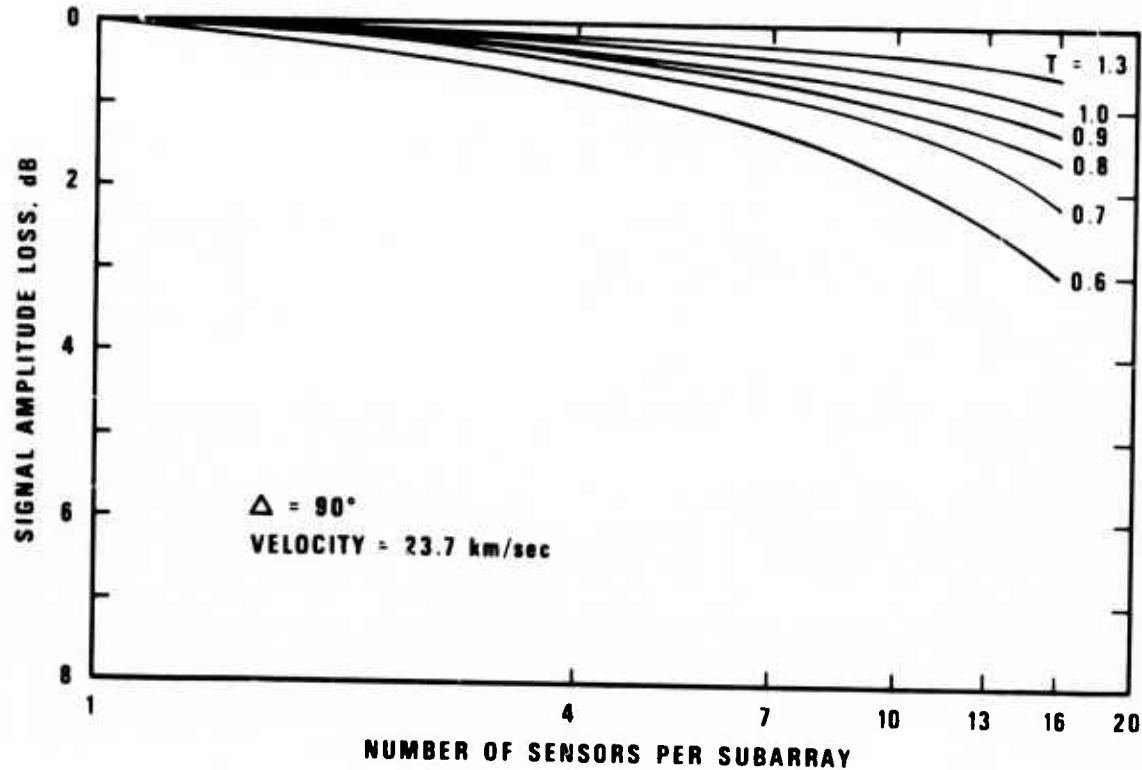


Figure 8. Theoretical signal loss for unphased sums as a function of number of sensors per subarray for several periods and for $\Delta = 90^\circ$.

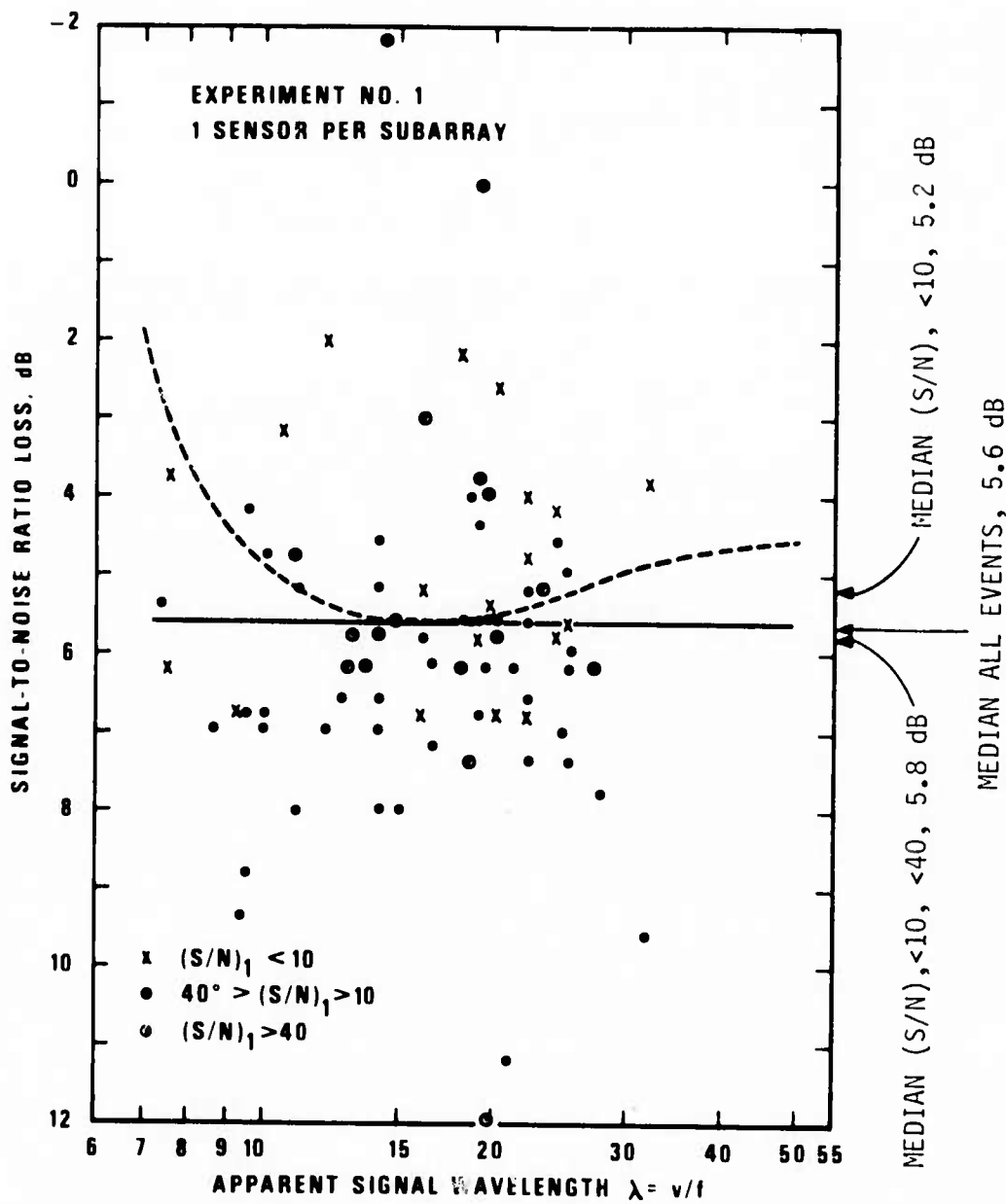


Figure 9. Signal-to-noise ratio loss in db as a function of apparent signal wavelength for experiment 1. The solid line is the (constant) array response of a single element shifted down until it passes through the median db point in the wavelength interval 12-18 km. The dashed line shows the response relative to a 15.5 km/sec beam directed at a 1 Hz signal.

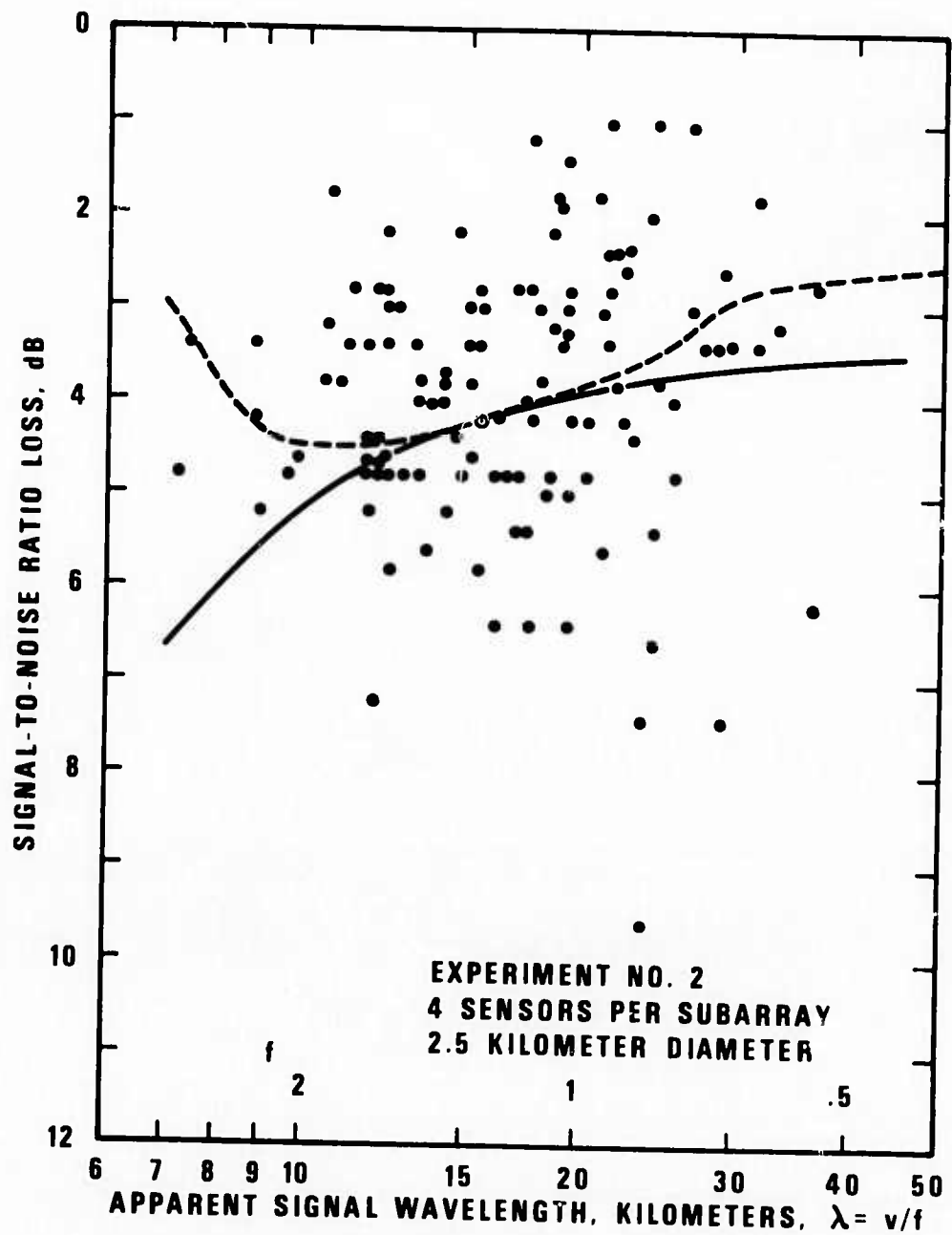


Figure 10. Signal-to-noise ratio loss in db as a function of apparent signal wavelength for experiment 2. The solid line is the array response of the inner 4 elements shifted down until it passes through the median db point in the wavelength interval 12-18 km. The dashed line shows the response relative to a 15.5 km/sec beam directed at a 1 Hz signal.

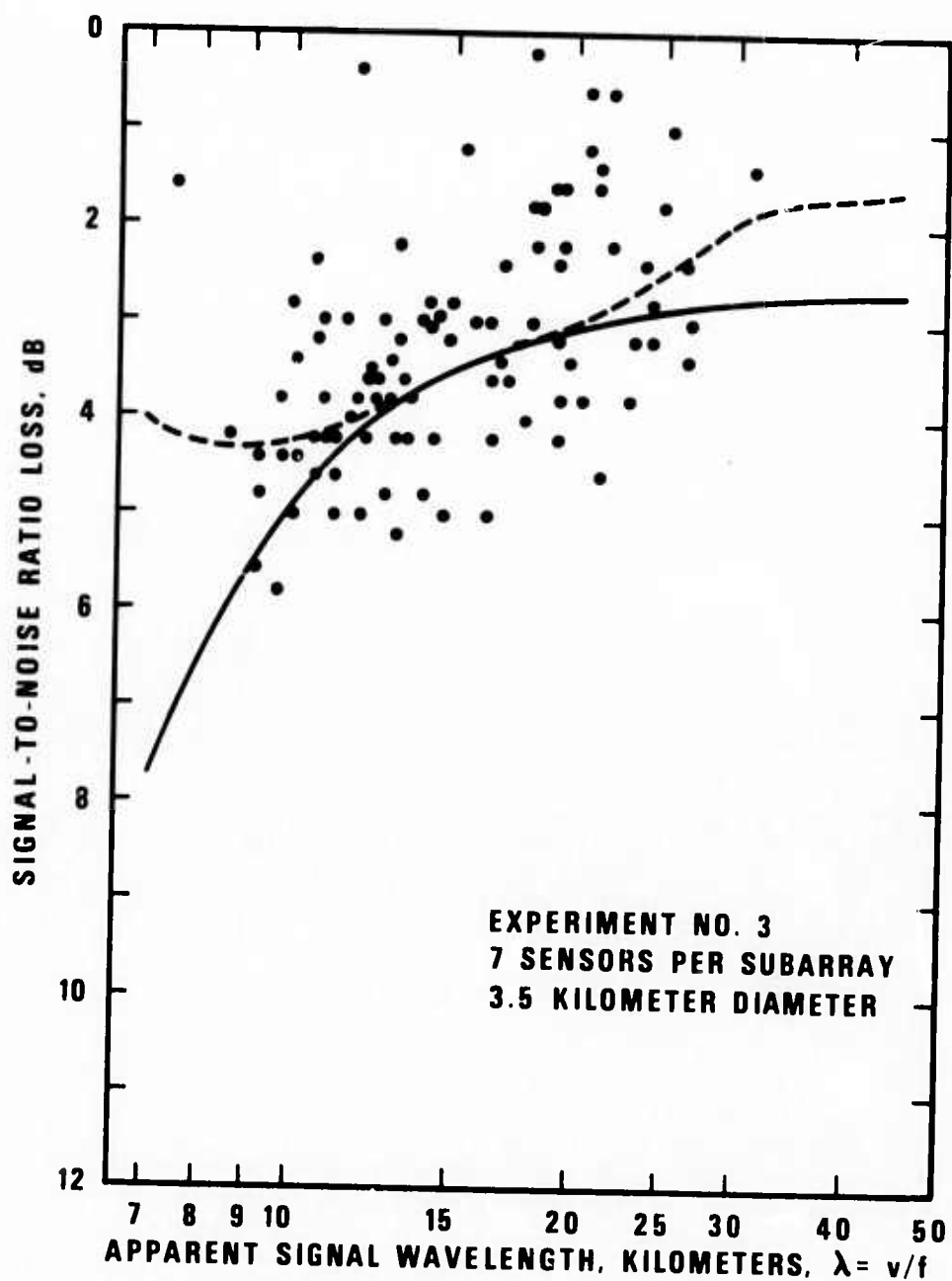


Figure 11. Signal-to-noise ratio loss in db as a function of apparent signal wavelength for experiment 3. The solid line is the array response of the inner 7 elements shifted down until it passes through the median db point in the wavelength interval 12-18 km. The dashed line shows the response relative to a 15.5 km/sec beam directed at a 1 Hz signal.

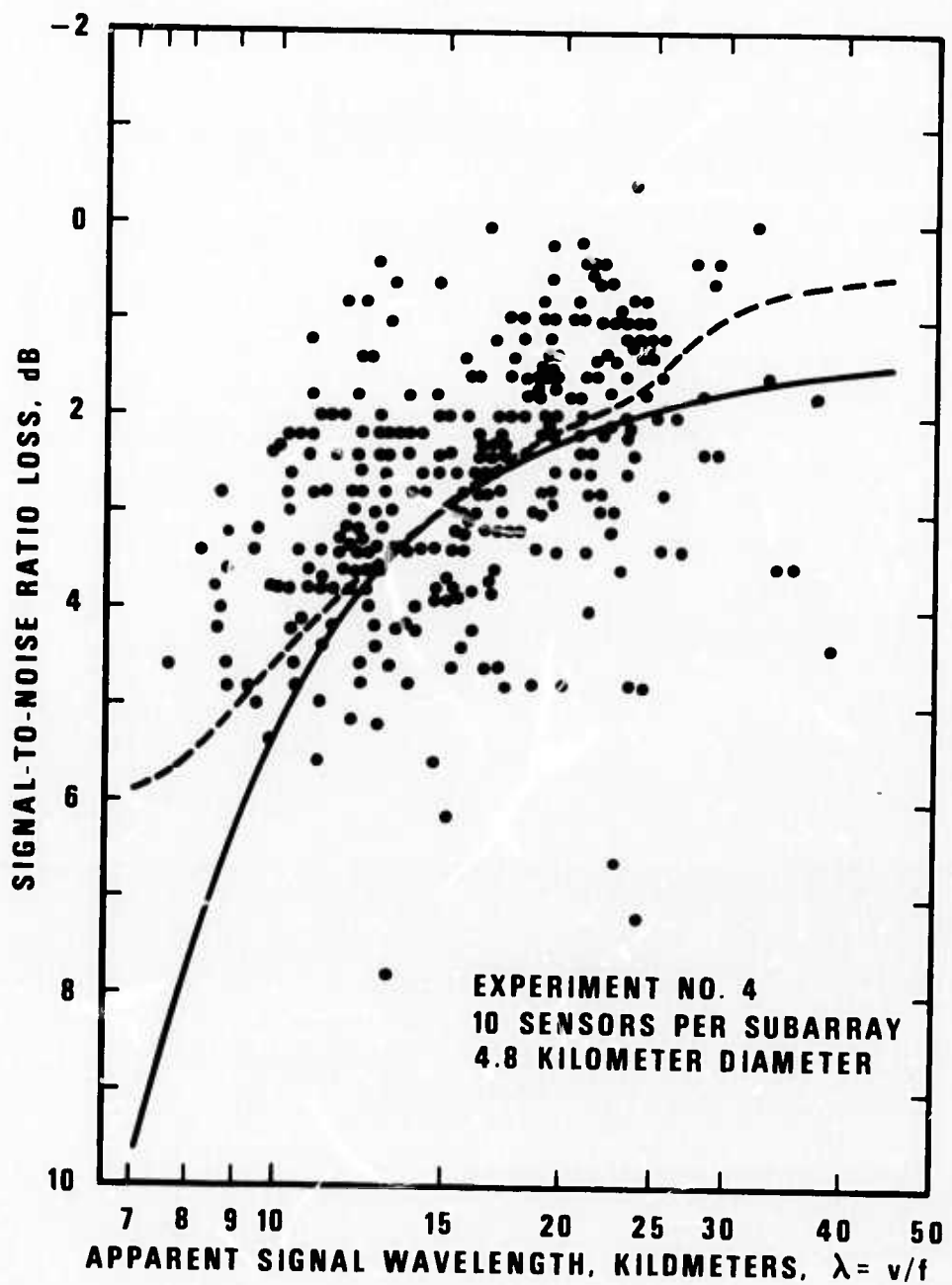


Figure 12. Signal-to-noise ratio loss in db as a function of apparent signal wavelength for experiment 4. The solid line is the array response of the inner 10 elements shifted down until it passes through the median db point in the wavelength interval 12-18 km. The dashed line shows the response relative to a 15.5 km/sec beam directed at a 1 Hz signal.

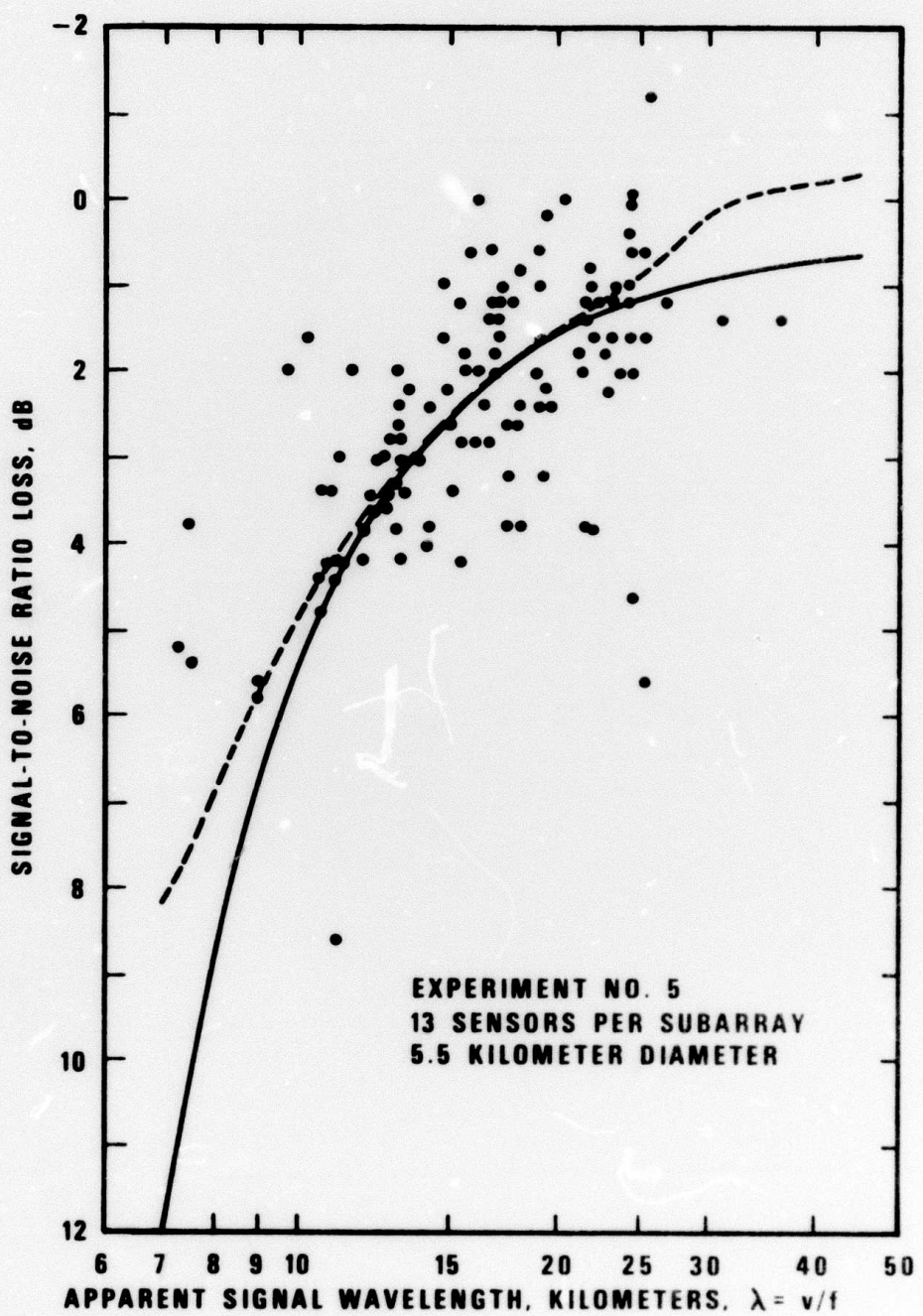


Figure 13. Signal-to-noise ratio loss in db as a function of apparent signal wavelength for experiment 5. The solid line is the array response for the inner 13 elements shifted down until it passes through the median db point in the wavelength interval 12-18 km. The dashed line shows the response relative to a 15.5 km/sec beam directed at a 1 Hz signal.

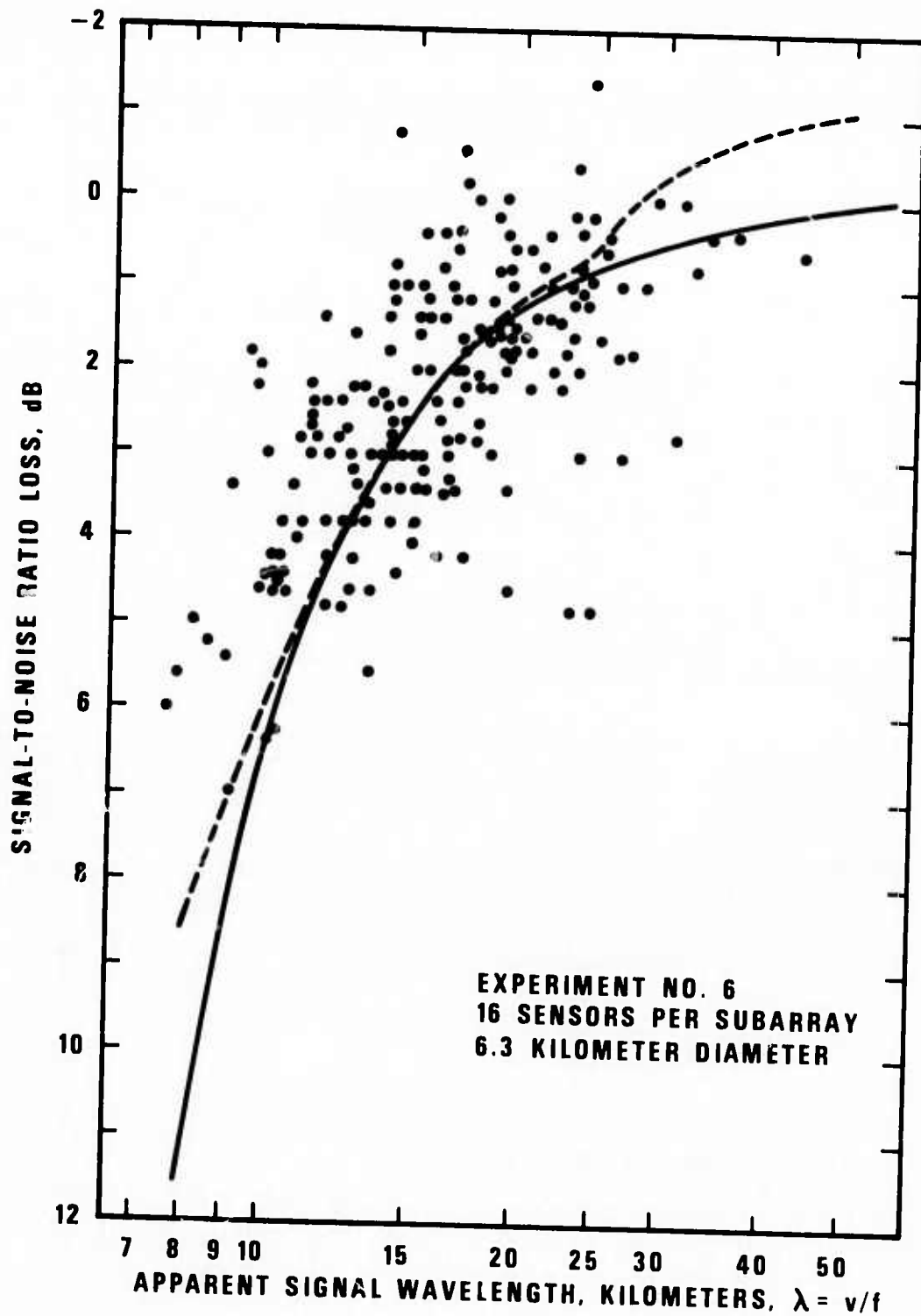


Figure 14. Signal-to-noise ratio loss in db as a function of apparent signal wavelength for experiment 6. The solid line is the array response of the inner 16 elements shifted down until it passes through the median db point in the wavelength interval 12-18 km. The dashed line shows the response relative to a 15.5 km/sec beam directed at a 1 Hz signal.

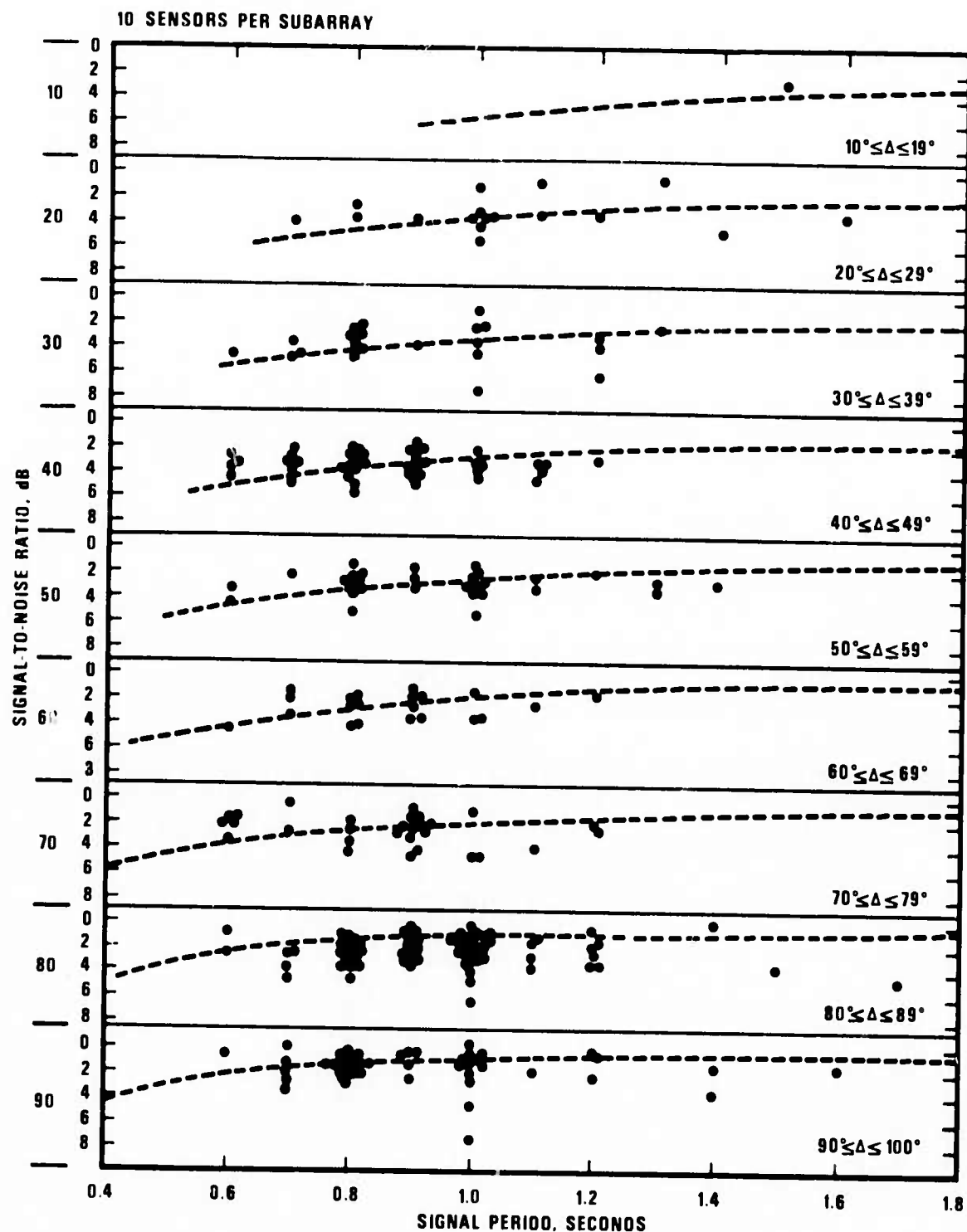


Figure 15. Signal-to-noise loss in db as a function of signal period for 9 distance intervals for experiment 4; 10 sensors per subarray. Line has been transformed from dashed line in Figure 12 by assuming loss at period T is equal to loss at $\lambda = vT$ where v is the wave velocity appropriate to the distance.

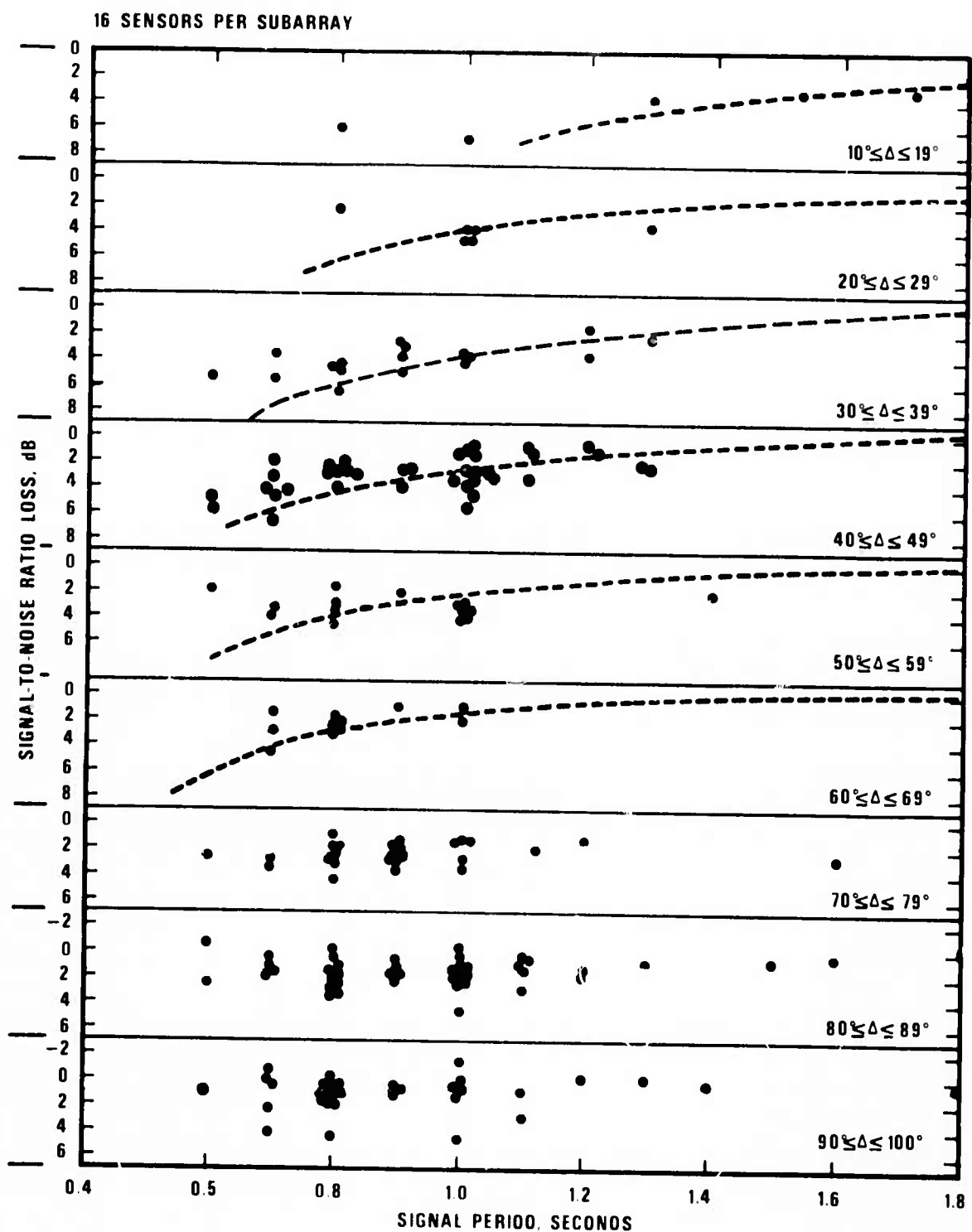


Figure 16. Signal-to-noise loss in db as a function of signal period for 9 distance intervals for experiment 6; 16 sensors per subarray. The dashed line has been transformed from the dashed line in Figure 14 by assuming loss at period T is equal to loss at $\lambda = vT$ where v is the wave velocity appropriate to the distance.

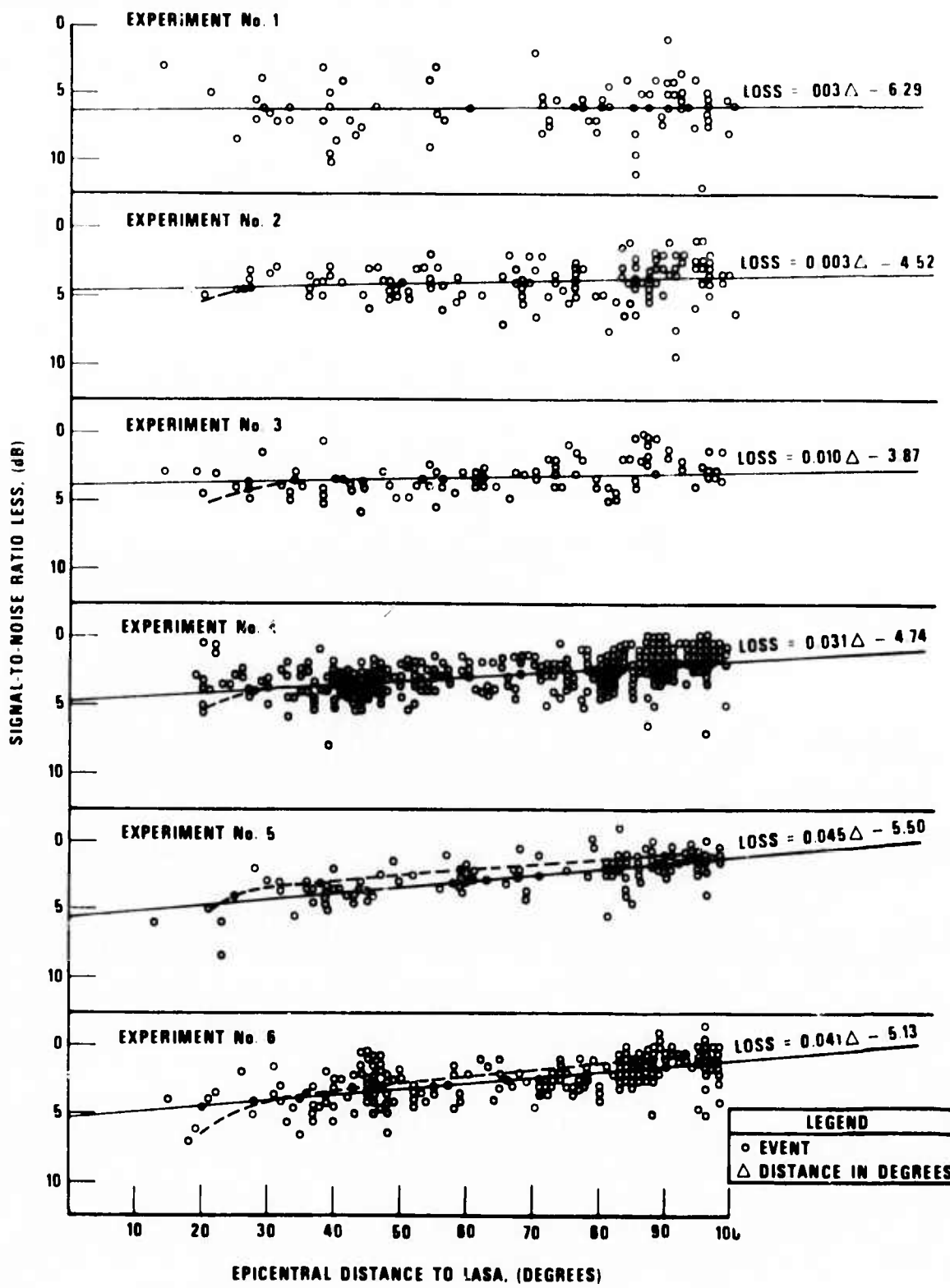


Figure 17. Plots of the signal-to-noise ratio losses for LASA beams containing unphased subarray sums as compared to those made up of phased subarray sums for each event versus epicentral distance for each experiment. Both regression lines and transformed dashed lines from Figures 9-14 with $f = 1.0$ have been drawn through the data. Transformation effected by assuming loss at distance Δ is equal to loss at $\lambda = vT$, $T = 1.0$, v as appropriate according to distance.

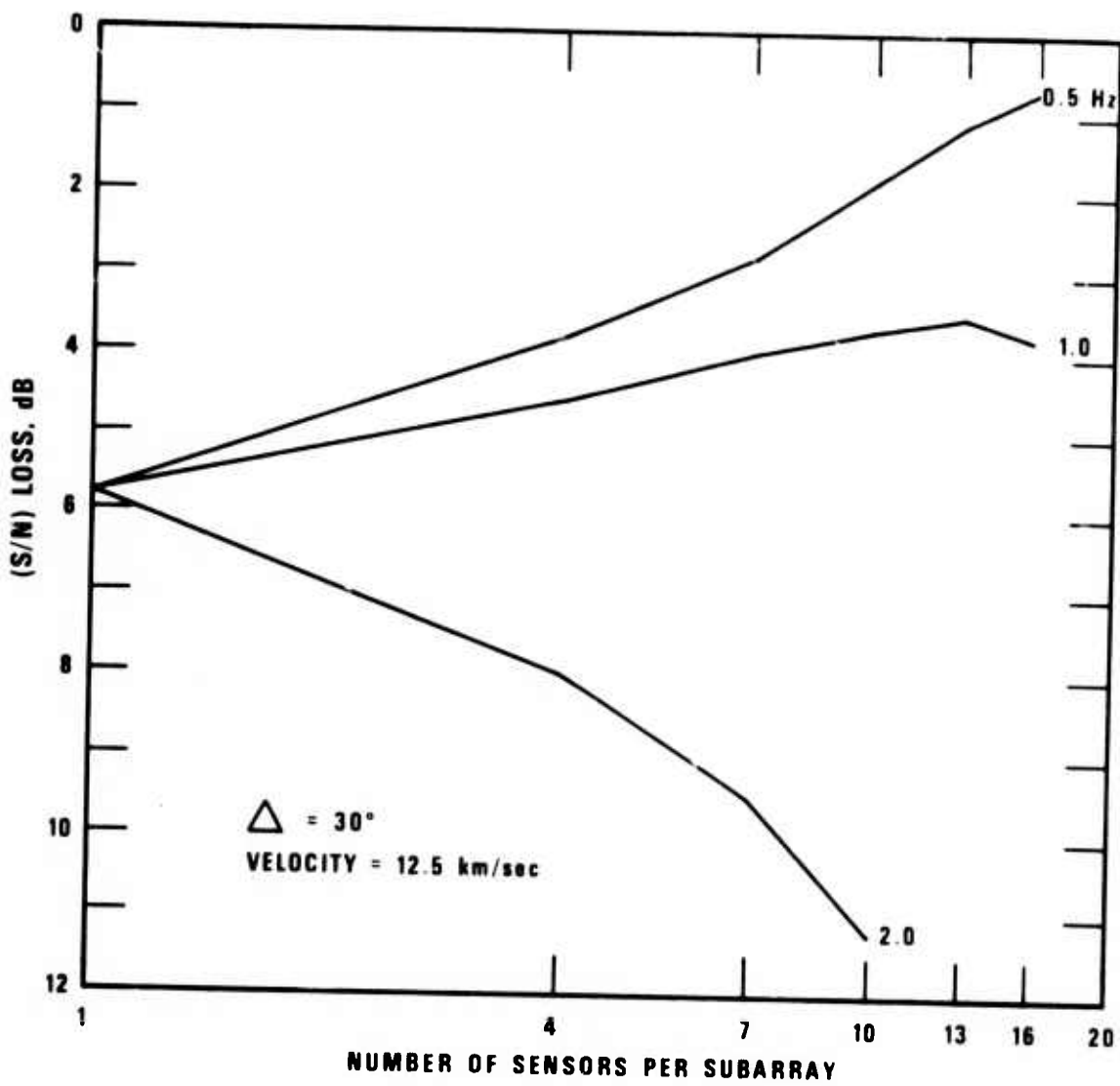


Figure 18. Signal-to-noise ratio loss for $\Delta = 30^\circ$ as a function of number of sensors per subarray for several frequencies. Taken from transformations of the dashed lines in Figures 9-14.

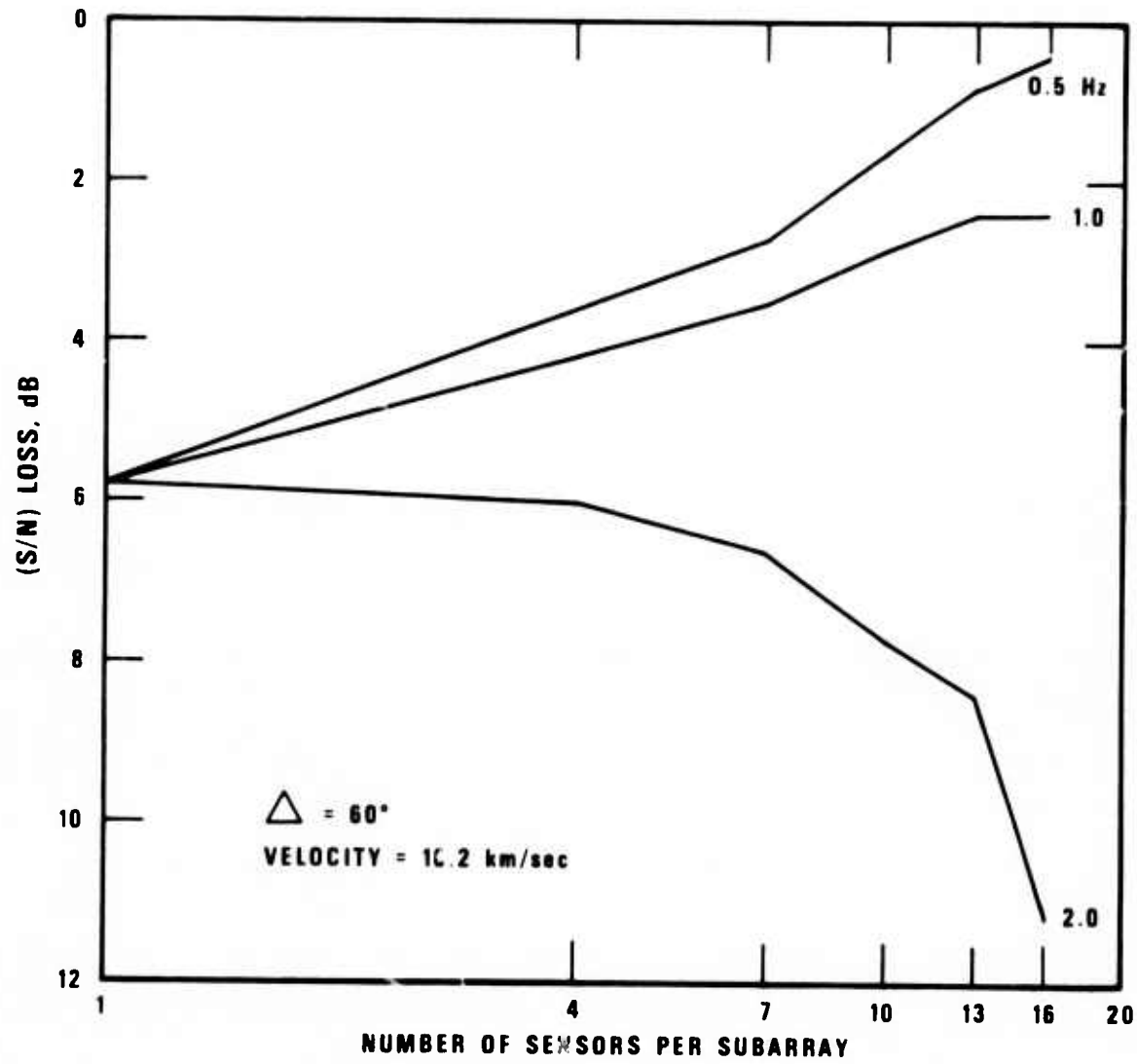


Figure 19. Signal-to-noise ratio loss for $\Delta = 60^\circ$ as a function of number of sensors per subarray for several frequencies. Taken from transformations of the dashed lines in Figures 9-14.

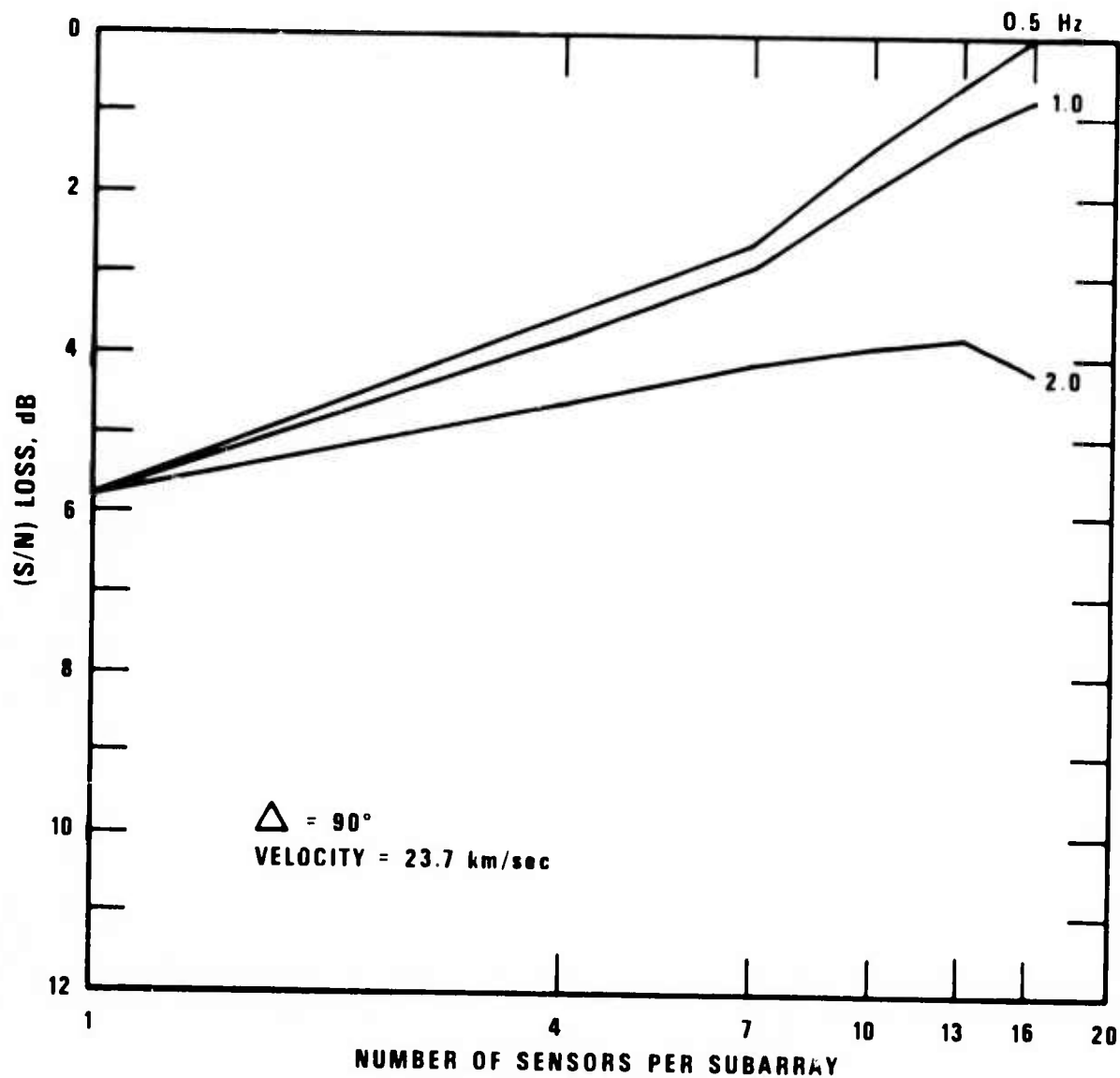


Figure 20. Signal-to-noise ratio loss for $\Delta = 90^\circ$ as a function of number of sensors per subarray for several frequencies. Taken from transformations of the dashed lines in Figures 9-14.

APPENDIX

DEVELOPMENT OF ARRAY LOSS EQUATION

Consider a sinusoidal seismic signal of frequency f , $Ae^{j\omega t}$, arriving at the center of the subarray at time t , thus the response of the i 'th seismometer is

$$Ae^{j\omega(t_o + \Delta t_i)}$$

where:

$$\Delta t_i = \frac{\vec{d}_i}{\vec{v}},$$

\vec{v} = apparent velocity, and

\vec{d} = distance vector from the center seismometer along the direction of wave propagation.

Therefore the response of the seismometer relative to the center seismometer at $t_o + \Delta t_i$ is :

$$R = \frac{Ae^{j\omega(t_o + \Delta t_i)}}{Ae^{jt_o}} = Ae^{j\omega\Delta t_i},$$

and the average response of the unphased subarray sum relative to the phased subarray sum is:

$$R = \frac{1}{N} \sum_{i=1}^N e^{j\omega\Delta t_i}, \text{ where,}$$

N = the number of sensors.

Then $R = \frac{1}{N} \sum_{i=1}^N (\cos \omega\Delta t_i + j \sin \omega\Delta t_i)$

$$= \frac{1}{N} \left(\sum_{i=1}^N \cos \omega\Delta t_i + j \sum_{i=1}^N \sin \omega\Delta t_i \right).$$

$$\begin{aligned}\text{Amplitude} &= \left\{ \left(\frac{1}{N} \sum_{i=1}^N \cos \omega \Delta t_i \right)^2 + \left(\frac{1}{N} \sum_{i=1}^N \sin \omega \Delta t_i \right)^2 \right\}^{1/2} \\ &= \left\{ \left(\frac{1}{N} \sum_{i=1}^N \cos 2\pi f \frac{d_i}{v} \right)^2 + \left(\frac{1}{N} \sum_{i=1}^N \sin 2\pi f \frac{d_i}{v} \right)^2 \right\}^{1/2}\end{aligned}$$

Let $\lambda = \frac{v}{f}$ = wavelength, then;

$$\begin{aligned}\text{Amplitude} &= \left\{ \left(\frac{1}{N} \sum_{i=1}^N \cos 2\pi d_i / \lambda \right)^2 + \left(\frac{1}{N} \sum_{i=1}^N \sin 2\pi d_i / \lambda \right)^2 \right\}^{1/2} \quad \text{and} \\ \text{and phase} &= \tan^{-1} \frac{\sum_{i=1}^N \sin 2\pi d_i / \lambda}{\sum_{i=1}^N \cos 2\pi d_i / \lambda}.\end{aligned}$$

To express the amplitude response in terms of db loss we have

$$\text{Loss(db)} = -20 \log_{10} \left\{ \left(\frac{1}{N} \sum_{i=1}^N \cos 2\pi d_i / \lambda \right)^2 + \left(\frac{1}{N} \sum_{i=1}^N \sin 2\pi d_i / \lambda \right)^2 \right\}^{1/2}.$$